MiniGraph: Querying Big Graphs with a Single Machine

Xiaoke Zhu[1,2], Yang Liu[1,2], Shuhao Liu[2], Wenfei Fan[2,3,1]
[1]Beihang University [2]Shenzhen Institute of Computing Sciences [3]University of Edinburgh
{zhuxk@,liuyang@act.}buaa.edu.cn,shuhao@sics.ac.cn,wenfei@inf.ed.ac.uk

ABSTRACT

This paper presents MiniGraph, an out-of-core system for querying big graphs with a single machine. As opposed to previous single-machine graph systems, MiniGraph proposes a pipelined architecture to overlap I/O and CPU operations, and improves multi-core parallelism. It also introduces a hybrid model to support both vertex-centric and graph-centric parallel computations, to simplify parallel graph programming, speed up beyond-neighborhood computations, and parallelize computations within each subgraph. The model induces a two-level parallel execution model to explore both inter-subgraph and intra-subgraph parallelism. Moreover, MiniGraph develops new optimization techniques under its architecture. Using real-life graphs of different types, we show that MiniGraph is up to 28.9× faster than prior out-of-core systems, and performs better than some multi-machine systems that use up to 12 machines.

1 INTRODUCTION

Big graph analytics has mostly been a privilege of big companies by employing a cluster of machines. For instance, to compute connected components of a graph with billions of vertices and trillions of edges, Google employs a 1000-node cluster with 12000 processors and 128 TB of aggregated memory [60]. To mine 3-FSM with support = 25000 on a million-edge graph, DistGraph [62] uses 128 IBM BlueGene/Q supercomputers and 32,768 GB memory. A number of graph systems have been developed to explore multi-machine parallelism, *e.g.,* [2, 24, 30, 32, 48, 52, 63, 66, 69, 72, 75]. However, big graph analytics via a cluster of machines is often beyond reach of small companies, which cannot afford such enterprise clusters.

Moreover, many parallel graph systems "have either a surprisingly large COST, or simply underperform one thread" [49]. For example, single-source shortest path (SSSP) is "essentially not scalable with an increasing number of machines" [67]. This is because multi-machine systems typically adopt the shared-nothing architecture, and the more machines are used, the heavier their communication cost is incurred. In addition, machines in such a system are often under-utilized due to unbalanced workload.

To rectify the limitations of the multi-machine systems, single-machine systems have been studied to explore multi-core parallelism, notably out-of-core systems to process data that is too large to fit into the main memory of a single machine at once [9, 29, 41, 47, 56, 68, 76]. The systems are developed on a machine that has a number of CPU cores, but limited memory capacity and disk I/O bandwidth. To get over the bottleneck, these systems have mostly focused on how to optimize I/O and memory efficiency.

Despite the efforts, disk I/O remains the bottleneck of the single-machine systems. Consider Weakly Connected Components (WCC). Given a graph G, WCC is to compute the maximum subgraphs of G in which all vertices are connected to each other via a path, regardless of the direction of edges. Consider GridGraph [76], a state-of-the-art out-of-core system featuring optimal I/O. We run the out-of-box WCC implementation of HashMin [70] that comes with GridGraph as a benchmarking application. The test was conducted on a workstation powered with a 10-core CPU with hyperthreading and 16 GB DDR4 memory. Graph G is `friendster` or `web-sk` [55]; both have ~1.8 billion edges, and amount to ~31 GB, about twice the memory size. We measure its system I/O using `iostat`. As shown in Table 1, while the two graphs are similar in size, GridGraph incurs drastically different I/O costs. It induces 2.7× disk read on `web-sk` as on `friendster`, which is relatively denser.

System	friendster (mean distance: 5.1)		web-sk (mean distance: 13.7)	
	# Supersteps	Disk Read	# Supersteps	Disk Read
GridGraph	21	135 GB	120	367 GB
MiniGraph	6	74 GB	9	82 GB

Table 1: WCC performance on GridGraph and MiniGraph.

An in-depth analysis reveals that the excessive I/O often stems from the vertex-centric model [30, 48, 76] adopted by GridGraph for parallel computation, referred to as VC. Under VC, an algorithm employs a user-defined function to process the immediate neighborhood of each vertex (or edge), and exchanges information between vertices via message passing. To send a message from a memory-resident vertex to a memory-absent one, it inevitably requires swapping their data in and out of the memory; as a consequence, VC generally incurs more disk I/O when G has a larger diameter.

Moreover, while VC is natural for graph algorithms such as PageRank [14] and HashMin [70] (for WCC), it is neither easy to write nor efficient to execute *e.g.,* an optimized WCC algorithm via Breath-First Search [34] and graph pattern matching algorithms with subgraph isomorphism or graph simulation [19] under VC.

Can we systematically reduce the I/O cost of an out-of-core graph system and improve multi-core parallelism? Given a computational problem, would other parallel models fit it better than VC?

MiniGraph. In an effort to answer these questions, we develop MiniGraph, an out-of-core system for graph computations with a single machine. Compared to the existing out-of-core single-machine graph systems, MiniGraph has the following features.

(1) A pipelined architecture. MiniGraph proposes an architecture that pipelines access to disk for read and write, and CPU operations for query answering. The idea is to overlap I/O and CPU operations, so as to "cancel" the excessive I/O cost. Moreover, this architecture decouples computation from memory management and scheduling, giving rises to new opportunities for optimizations.

(2) A hybrid parallel model. MiniGraph extends the graph-centric model (GC) of [24] from multiple machines to multiple cores. GC allows a core to operate on a subgraph at a time, speed up beyond-neighborhood computation and reduce its I/O; it also simplifies parallel programming by parallelizing existing sequential algorithms across cores. MiniGraph also proposes a hybrid model for VC and GC, and a unified interface such that the users can benefit from both

and can choose one that fits their problems and graphs the best.

As shown in Table 1, when computing WCC over `friendster` (resp. `web-sk`), the benefit of the beyond-neighborhood computation (GC) is evident: MiniGraph (a) takes 6 (resp. 9) supersteps to converge under the bulk asynchronous model (BSP) [64], as opposed to 21 (resp. 120) steps with GridGraph; (b) reads 74 GB (resp. 82 GB) of data in contrast to 135 GB (resp. 367 GB) of GridGraph; and (c) is less sensitive to the distribution of the input graphs.

(3) Two-level parallelism. The hybrid model also enables two-level parallelism: inter-subgraph parallelism via high-level GC abstraction, and intra-subgraph parallelism for low-level VC operations. This presents new opportunities for improving multi-core parallelism. However, its relevant scheduling problem is NP-complete. This said, we develop an efficient heuristic to allocate resources, which is dynamically adapted based on resource availability.

(4) System optimizations. MiniGraph develops unique optimization strategies enabled by the hybrid parallel model. It employs a lightweight state machine to model the progress of cores working on different subgraphs, and tracks messages between cores. These allow it to explore shortcuts in the process to avoid redundant I/O.

Contributions & organization. After reviewing VC and GC parallel models (Section 2), we present MiniGraph as follows:

- its pipelined architecture and a system overview (Section 3);
- the hybrid parallel model and case studies (Section 4);
- the two-level parallel execution model (Section 5);
- implementation and optimization (state machine, Section 6); and
- an experimental study (Section 7). Using real-life graphs, we find the following. (a) With various out-of-core workloads, MiniGraph outperforms prior out-of-core systems by 6.9× on average, up to 28.9×. (b) It is able to query a graph of size 10× of the memory capacity. (c) It outperforms the state-of-the-art multi-machine systems when they use up to 12 machines.

Related work. We classify prior parallel graph systems as follows.

Multi-machine systems. A number of multi-machine systems have been developed, to support big graph analytics by scaling out, *e.g.,* [2, 17, 24, 30, 32, 48, 52, 63, 66, 69, 75, 75]. Such systems adopt a shared-nothing architecture: they partition the input graph, and distribute the fragments to workers; all workers process their local fragments in-memory in parallel, and communicate with each other via message passing. Most of these systems adopt the VC model, except that GRAPE [24] proposes and supports GC. GraphScope [4, 20] extends GRAPE and supports a unified interface for VC and GC.

In contrast to scaling out with multiple machines, (1) MiniGraph uses a single machine and explores multi-core parallelism. It aims to provide small businesses with a capacity of big graph analytics under limited resources. (2) It adopts a shared-memory multi-core architecture and employs the secondary storage as the memory extension. While the communication cost of multi-machine systems hampers their scalability when adding more machines [3], a major challenge to out-of-core single machine systems such as MiniGraph is the I/O cost. (3) It proposes a hybrid parallel programming model and a two-level parallel execution model to support VC and GC.

Single-machine in-memory systems. When graphs are small enough to fit into the memory of a single machine, in-memory systems [46, 53, 57, 71, 73] aim to conduct computations with high performance. Such systems focus on optimization techniques on memory-resident graphs, *e.g.,* efficient task parallelization [53, 57, 73] and improved data locality [71]. Ligra [57] introduces a variant of VC model that allows user-specified parallelization of operations. Polymer [71] is designed for a NUMA architecture, where the memory access latency of a processor is not uniform across the address space.

In contrast, MiniGraph targets large graphs that exceed the memory capacity of a single machine. It performs iterative out-of-core computation, by actively swapping graph data between the memory and the disk. It deals with inevitable and possibly prohibitive I/O costs, a challenge that is not encountered by in-memory systems.

Single-machine out-of-core systems. Closer to this work are out-of-core systems [9, 29, 41, 47, 56, 65, 68, 76]. Most of the systems adopt VC and BSP. The techniques have mostly focused on reducing I/O, the major performance bottleneck. XStream [56] proposes stream reading of edges to maximize sequential disk accesses. GraphChi [41] divides the input data into small shards, each having a disjoint set of independent edges; it employs Parallel Sliding Windows such that shards in the window are allowed in memory, while those being pushed out are written onto the disk. Vora *et al.* [65] propose online adjustment of sharding, which avoids loading unneeded edges at the price of extra computation. GridGraph [76] improves the locality of edge sharding via 2-level partitioning based on source and destination IDs, and enables selective scheduling of data. Clip [9] allows asynchronous and repetitive processing of an in-memory shard; however, it must be explicitly invoked by users in their VC code, which might be error-prone. With extra hardware, Gill *et al.* [29] use persistent memory sticks as memory extension, which have higher throughput than SSDs (Intel has discontinued the Optane-only SSDs for the consumer market [58]). Mosaic [47] employs an Intel Xeon Phi coprocessor to accelerate CPU computations.

In contrast, MiniGraph (1) introduces a pipelined architecture to "cancel" the I/O costs; (2) it supports both GC to parallelize existing sequential algorithms and speed up beyond-neighborhood computation, and VC to parallelize edge/vertex operations in each subgraph; (3) it proposes a two-level execution model to support inter-subgraph and intra-subgraph parallelism; and (4) it develops new optimization strategies to reduce I/O. (5) As opposed to [29, 47], MiniGraph requires no dedicated hardware for storage or computation; it assumes an off-the-shelf machine that can be easily acquired.

Polyglot systems. Polyglot systems [15, 16, 18, 36, 37, 45, 59, 61, 74] take graphs as edge relation views, and cast graph queries into SQL, which requires large memory for intermediate data. In contrast, MiniGraph is a native graph system. It uses a single machine with limited memory, which is often insufficient for polyglot systems.

2 BACKGROUND AND MOTIVATION

In this section, we review parallel graph (programming) models.

Consider graph $G = (V, E, L)$, directed or undirected, where V is a finite set of vertices; $E \subseteq V \times V$ is a set of edges; each vertex v in V (resp. edge $e \in E$) carries label $L(v)$ (resp. $L(e)$) for properties.

In principle, a graph parallel model determines how users can program with the system and how the programs are executed in parallel. Two types of parallel models have been implemented in (multi-machine) graph systems, namely, VC and GC.

The vertex-centric model (VC). Initially proposed by Pregel [48], VC has been the *de facto* go-to model for parallel graph systems. Its principle is for users to think like a vertex: a vertex program is "pivoted" at a vertex; it may only directly access information at the current vertex and its adjacent edges [30, 48]; information is exchanged between "remote" vertices via message passing. Several variants of VC are in place. For example, the GAS model of PowerGraph [30] requires three user-specified functions: (1) Gather defines how a vertex v aggregates incoming messages from its neighbors; (2) Apply specifies how v updates its own attributes based on the message received; and (3) Scatter defines what messages at v are generated as outgoing messages to its neighbors.

It is natural to program with VC for problems when its computation can be distributed to vertices and is centered at each vertex, such as PageRank. It is, however, nontrivial to write VC algorithms for problems that are constrained by "joint" conditions on multiple vertices, *e.g.,* graph simulation [50] and subgraph isomorphism [28]. While a variety of conventional sequential algorithms have been developed for such problems, to program with VC, one has to recast the existing algorithms into the VC model. Moreover, such VC programs are often inefficient since they incur heavy message passing. The issue is more staggering for out-of-core systems since we have to repeatedly load the adjacent list of a vertex from disk to memory when the recursive/induction process backtracks.

Example 1: As a common benchmarking algorithm for WCC, HashMin works as follows under VC: (1) initially, each vertex is assigned a distinct numeric label; (2) in every iteration, each vertex collects the labels from its neighbors (via bi-directional message passing along edges), and updates its own label with the minimum within the neighborhood; (3) when no more label updates can be made, it returns the total number of distinct labels in the graph.

On graph G of Figure 1a, HashMin takes 5 supersteps under BSP as shown in Figure 1b, where active vertices are in light color and inactive ones are in gray. We also count the number of message passed in each superstep, marked as "#Ops". As the computation progresses, more vertices become inactive, and less messages are passed.

Observe the following: (1) The labels of vertices in Subgraph D are overwritten repeatedly; many initial messages and label updates are redundant. In total 92 messages are passed, while G has 16 edges only. (2) It takes 5 supersteps. Every edge must be swapped in and out of the memory for 5 times if G cannot fit in the memory entirely. It is translated to a disk read demand that is 5× of the size of G. □

The graph-centric model (GC). Proposed by GRAPE [24], GC carries out data-partitioned parallelism. Given a big graph G, it partitions G into fragments (subgraphs) using existing graph partitioners (edge-cut [10, 38], vertex-cut [13, 30, 39] or hybrid [21]), and distributes the fragments to different workers. It parallelizes sequential graph algorithms. More specifically, for a graph computational problem Q, users may provide three (existing) sequential algorithms PEval, IncEval and Assemble, referred to as a PIE program:

- PEval is a conventional algorithm for Q such that all workers execute it on their local fragments in parallel, and produce partial results (*partial evaluation*); the values of border nodes (*e.g.,* vertices with edges to other fragments) are exchanged as messages;
- IncEval is a sequential incremental algorithm for Q; it is repeatedly executed to refine the partial results by treating messages from other workers as updates (*incremental computation*); and
- when no more messages are exchanged, Assemble aggregates partial results from all the workers and forms the final answer.

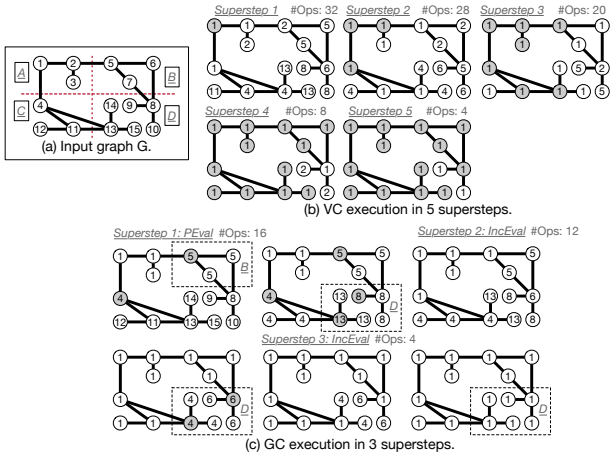

Figure 1: WCC computation on G with VC or GC.

The parallelized computation starts with PEval, and is followed by iterative IncEval until a fixpoint is reached. Under a generic condition, it guarantees to converge at correct answers as long as the sequential algorithms PEval, IncEval and Assemble are correct [25]. All three functions operate on subgraphs of graph G.

As opposed to VC, GC supports beyond-neighborhood computations. It simplifies parallel programming by parallelizing existing sequential algorithms; moreover, it reduces unnecessary recomputation via iterative IncEval. However, for problems such as PageRank, when graph partitions are not "well balanced" [21], the communication cost of a GC algorithm between workers may be higher than its VC counterpart. Moreover, the parallelism is explored at the subgraph level, not at the vertex/edge-level in each subgraphs.

Example 2: As opposed to HashMin, GC parallelizes a more efficient sequential WCC algorithm. After labeling all vertices of graph G with distinct integers, the algorithm proceeds on each fragment (subgraph) F_i of G with single-threaded worker W_i. (1) Starting with PEval, W_i initiates BFS from the vertex v that has the minimum label $L(v)$ among all the vertices in F_i. During the BFS, it overwrites their labels with $L(v)$. (2) As soon as no vertex remains active, W_i generates messages comprising the updated labels of border nodes of F_i. (3) With all updates received from other workers, if v's update carries a smaller label, W_i overwrites $L(v)$; it invokes IncEval to incrementally refine the partial results until no message is exchanged among workers. (4) Finally, the algorithm calls Assemble to count WCC as the total number of distinct labels from all workers.

Suppose that graph G is partitioned into 4 subgraphs, as depicted in Figure 1a. GC completes WCC in 3 supersteps under BSP (1 round of PEval and 2 rounds of IncEval), as illustrated in Figure 1c.

Observe the following: (1) GC reduces redundant computation and needs 3 supersteps only. (2) It passes 32 messages on G (-65% from VC), and requires loading each subgraph only three times (-40% from VC). This said, the computation within each subgraph is conducted *sequentially*, and there is room for improvement. □

To the best of our knowledge, no single-machine systems supports the GC model despite its efficiency and ease of programming.

3 MINIGRAPH: AN OVERVIEW

In this section, we present an overview of MiniGraph. Unlike prior single-machine graph systems, MiniGraph takes a unique approach by proposing a pipelined architecture, a hybrid parallel model for VC and GC, and two-level (inter/intra-subgraph) parallelism.

Graph partitioning. Previous single-machine systems organize an input graph as a large number of chunks (*a.k.a.* shards [41], blocks [76]), each consisting of a (possibly small) list of edges. This design serves the sole purpose of gathered I/O, while the system schedules and operates directly on edges. it provides fine-grained scheduling, yet may not work well with the block storage.

MiniGraph explores a conceptually different approach. It partitions a large graph G such that one or more fragments can fit into the memory. A fragment is essentially a *subgraph* of G. MiniGraph adopts a two-level abstraction: (1) at a high level, it sees a subgraph as the atomic unit for scheduling and I/O; and (2) when processing a subgraph that is in memory, it may carry out parallel computation on the edges and vertices. Our empirical study shows that the two-level abstraction improves multi-core parallelism.

MiniGraph may use any graph partitioners designed for multi-machine parallel systems (*e.g.,* [10, 13, 21, 30, 38, 39]).

A pipelined architecture. MiniGraph takes as input the subgraphs (fragments) $F_0, F_1, \ldots, F_{n-1}$ of a (possibly large) G; the subgraphs are initially stored on disk. MiniGraph iteratively processes the subgraphs in a pipelined architecture, as shown in Figure 2.

More specifically, MiniGraph breaks down the out-of-core processing of a subgraph F_i into three consecutive stages: (1) read F_i into the memory, (2) compute and update F_i, and (3) if necessary, write the updated F_i back to the secondary storage. It has three components: Loader, Evaluator, and Discharger, for the three stages, respectively. They work asynchronously in a pipeline, and are loosely coupled via two task queues InboundQueue and OutboundQueue.

Loader. Working in a dedicated thread, Loader continuously selects and reads a memory-absent subgraphs from disk into the memory, as long as system memory capacity is not exhausted. It operates regardless of the progress of other system components. This design makes full utilization of disk read bandwidth. Instead of many scattered reads, Loader issues a small number of bulk read requests, which can improve read throughput and reduce system interrupts.

Once a subgraph F_i is loaded into the memory, Loader pushes its token T_i into InboundQueue, where T_i includes metadata of F_i such as pointers to the data and its current state.

Evaluator. As the downstream component of Loader, Evaluator is responsible for efficient execution of an application. It pops token T_i from InboundQueue, locates F_i in memory, and initializes a virtual worker W_i with reserved thread allocations to execute the program on F_i. During the execution, W_i can update F_i in place, and may generate updates to other subgraphs. The update messages are cached in MessageStore, an array-like storage in memory.

To fully exploit the multi-core parallelism and cache locality, Evaluator manages a global thread pool, whose size is decided by the system hardware concurrency. Whenever threads become idle, it triggers Scheduler, which re-allocates the resources to workers (see below). Once a worker completes, Evaluator reclaims the reserved threads and pushes token T_i to OutboundQueue for discharging.

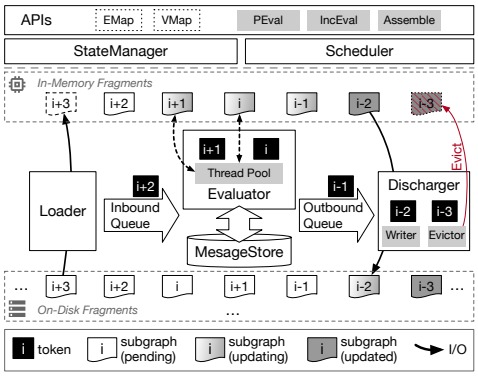

Figure 2: The pipelined architecture of MiniGraph.

Discharger. As a counterpart of Loader, Discharger writes the subgraph data back to the disk. It consumes OutboundQueue continuously in a dedicated thread. For a popped token T_i, it (1) writes the updated F_i contiguously to disk, and (2) records F_i's latest state to StateManager for maintenance. After F_i is fully discharged, Discharger evicts it from memory and reclaims space for Loader.

Key modules. MiniGraph implements the following unique modules for programming, execution and optimization.

APIs for a hybrid parallel model. MiniGraph exposes PIE+, a unified interface that integrates VC with GC programming (see Section 4). Users can not only parallelize sequential graph algorithms under GC to simplify parallel programming, but also further explore intra-subgraph parallelism under VC via the new interfaces.

Scheduler. Scheduler tracks and allocates threads in ThreadPool in which each thread corresponds to a physical CPU core. It makes decisions to assign physical threads to virtual workers to carry out (parallel) computations on fragments. It also makes active adjustments to support two-level parallelism: when a thread is available, Scheduler allocates it to either a new worker by consuming InboundQueue for speeding up inter-subgraph parallelism, or a running worker for improving intra-subgraph parallelism.

StateManager. As computation progresses on the subgraphs of G, StateManager maintains a state machine to model their status. It is a low-cost method for convergence detection, and it helps identify chances to skip redundant I/O or computation.

We will present the details of the hybrid parallel model, two-level parallelism and state manager in Sections 4–6, respectively.

4 HYBRID PARALLEL MODEL

In this section we introduce the hybrid parallel model of MiniGraph. We present its programming interface PIE+ (Section 4.1), followed by case studies to illustrate how to program with PIE+ (Section 4.2).

4.1 The Hybrid Parallel Model and its APIs

The hybrid model of MiniGraph aims to improve multi-core parallelism by supporting inter-subgraph and intra-subgraph parallelism.

Overview. Given a graph computational problem Q and a graph G, MiniGraph processes subgraphs $F_0, F_1, \ldots, F_{n-1}$ of G. It assigns virtual worker W_i to F_i ($i \in [0, n-1]$). To simplify the discussion, we adopt BSP [64] for synchronization. In each superstep, each fragment is processed exactly once. When F_i is loaded into the

Algorithm 1: A conceptual implementation of EMap

Scope Variables: local subgraph F_i, intermediate data Π_i.
Input: active vertex set $\Delta \in 2^V$, update function $f_E : (V, V) \to 2^V$.
Output: updated active vertex set $\Delta' \in 2^V$.

```
1 Δ' := ∅;
2 foreach u in Δ do in parallel
3     foreach v in u.neighbors do in parallel
4         Δ' := Δ' ∪ f_E(u, v)        /* F_i and Π_i may be accessed. */
5 return Δ';
```

Algorithm 2: A conceptual implementation of VMap

Scope Variables: local subgraph F_i, intermediate data Π_i.
Input: active vertex set $\Delta \in 2^V$, update function $f_V : V \to 2^V$.
Output: updated active vertex set $\Delta' \in 2^V$.

```
1 Δ' := ∅;
2 foreach u in Δ do in parallel
3     Δ' := Δ' ∪ f_V(u)           /* F_i and Π_i may be accessed. */
4 return Δ';
```

Algorithm 3: PEval for WCC under PIE+.

Input: subgraph $F_i = (V_i, E_i, L_i)$.
Output: set CC_i of connected components in F_i.

```
Message Preamble:        /* candidate set C_i includes all border nodes. */
    VMap (V_i, function (v) { v.root := v; return ∅; }) ;
1 CC_i := ∅; Π := V_i;          /* Π is the set of unvisited vertices. */
2 while Π not empty do
3     find root vertex v_r, such that L_i(v_r) = min_{u∈Π} L_i(u);
4     CC_i := CC_i ∪ {v_r}; remove v_r from Π;
5     Δ := {v_r};
6     while Δ not empty do Δ := EMap (Δ, BFSRecur);
7 return CC_i;
Message Segment: M_i := {(v, L_i(v.root)) | v ∈ C_i}; f_aggr := min;
8 Procedure BFSRecur (u, v) :
9     if v not in Π then return ∅;
10    remove v from Π; v.root := v_r;
11    return {v};
```

memory, W_i is activated and allocated CPU resources by Scheduler.

Recall from Section 2 that under GC, users provide a PIE program for Q, which consists of three sequential algorithms PEval, IncEval and Assemble. Each worker W_i executes PEval on its local subgraph F_i for partial evaluation; it then iteratively and incrementally refines the partial results via IncEval on F_i by treating messages between workers as updates, until it reaches a fixpoint, followed by Assemble to aggregate the partial results from all workers into the final answer. In principle, each W_i runs PEval and IncEval *sequentially*.

The key idea of the hybrid parallel model is two-level parallelism. At the top level, it adopts GC to benefit from data-partitioned inter-subgraph parallelism, parallelize existing sequential graph algorithms, and speed up beyond-neighborhood computations. Moreover, within each subgraph, it parallelizes the execution of PEval and IncEval by enforcing VC; that is, once a subgraph is in memory, it leverages the shared-memory architecture of a single machine and promotes intra-subgraph vertex/edge-level parallelism via VC.

Example 3: Continuing with Example 2, consider the execution of the WCC algorithm under GC. On subgraph A, it initiates BFS from root vertex with an initial label 1. It recurses as two independent BFSes starting from both neighbors of vertex 1, *i.e.,* vertices 2 and 4, which then proceed as BFSes from vertices 11 (subgraph C), 13 (subgraph B), and 5 (subgraph D), so on and so forth. If we execute each recursion with 2 parallel threads, we can get a 2× speedup. □

PIE+. In light of this, we propose a new programming interface, called PIE+. Given a problem Q, MiniGraph also takes algorithms PEval, IncEval and Assemble for Q, and follows the same workflow of GC for inter-subgraph parallelism. Moreover, it extends PIE with two additional primitives, EMap and VMap, along the same lines as the VC interface of Ligra [57]. These primitives make PEval and IncEval parallel within each subgraph at the edge/vertex level.

EMap and VMap work on a set Δ of "active" vertices, which are to be further processed. Intuitively, EMap and VMap implement flatMap of functional programming, to execute an update function at each active vertex v in Δ and moreover, "flat map" v to a new set of vertices that will remain active or get activated after the operation.

As shown in Algorithm 1, EMap takes as input Δ and an edge update function f_E. For each active vertex u in Δ, EMap makes updates along each of u's outgoing edge by applying f_E, executed in parallel. Here f_E is a user-defined function. It processes an edge $e = \langle u, v \rangle$ from u, makes updates based on the data associated with e, u and v, and returns a new (possibly empty) set of vertices that remain active after the update. Moreover, f_E may access the local subgraph F_i and intermediate data structure Π_i of PEval and IncEval.

Similarly, VMap takes Δ and a vertex update function f_V as input. As shown in Algorithm 2, it aims to parallelize operations that are centered at each active vertex in Δ. Instead of working along edges, f_V operates on each vertex $u \in \Delta$, processes and updates u by accessing F_i and Π_i, and returns an updated active vertex set.

Message passing. Similar to GC, PIE+ approaches inter-subgraph synchronization via message passing. At each subgraph F_i, it declares (a) *status variables* $\bar{x}$ for its *border nodes*, *i.e.,* vertices that have edges to other fragments (under edge-cut); and (b) an aggregate function f_{aggr}, *e.g.,* min and max. Intuitively, the status variables are candidates to be updated by the incremental step of IncEval, and f_{aggr} resolves conflicts when multiple workers assign different values to the same variable $v.\bar{x}$ for a border node v of F_i.

MiniGraph adopts a *push-pull* mechanism for workers to exchange messages through MessageStore. Right after worker W_i gets initialized, it checks MessageStore to *pull* a set M_i of messages, which consists of updated status of the border nodes in F_i. After concluding computation, W_i collects the latest values $v.\bar{x}$ for each border node v, and *pushes* them into MessageStore for aggregation. It inserts $\bar{x}$ to MessageStore$[v]$ if the entry is missing, and applies $f_{\text{aggr}}(\text{MessageStore}[v], \bar{x})$ to resolve the conflict.

Example 4: We present a PIE+ program for WCC. It is the same as the PIE program of [25] for WCC, except that it parallelizes BFSes in PEval and IncEval within each subgraph via EMap and VMap. We consider *w.l.o.g.* edge-cut partitions [10, 38], in which border vertices are those that have edges to another fragment.

(1) PEval. As shown in Algorithm 3, at worker W_i, PEval computes the connected components CC_i of its local subgraph F_i, the partial result at F_i. Here CC_i is the set of root vertices that identify connected components, referred to as *CRoots*. It declares (a) a link to its CRoot, and (b) min as f_{aggr}. PEval (a) initializes an empty CC_i and a set Π of unvisited vertices in F_i (Line 1); and (b) conducts iterative

Algorithm 4: IncEval for WCC under PIE+.

Input: subgraph $F_i = (V_i, E_i, L_i)$, CC_i, incoming messages M_i.
Output: refined set CC_i of connected components in F_i.

1 $\Delta = \{v \mid v \in M_i\}$; VMap($\Delta$, UpdateRoot);
2 **return** refine(CC_i); /* merge roots with the same label in CC_i. */
Message Segment: $M_i := \{(v, L_i(v.\text{root})) \mid v \in C_i\}$;
3 **Procedure** UpdateRoot (v) :
4 $v_r := v$.root;
5 **while** v_r not in CC_i **do** $v_r := v_r$.root;
6 update v.root $:= v_r$; $L_i(v_r) := \min(L_i(v_r), M_i[v])$;
7 **return** $\emptyset$;

BFS until all vertices are visited, *i.e.,* Π is emptied (Line 2–6). The BFS finds its CRoot v_r at the vertex with the lowest label (Line 3), adds v_r to CC_i to identify a unique connected component (Line 4), and sets the label of each descendant of v_r to the label $L_i(v_r)$ of the CRoot (Line 5–6). MessageStore packs the smallest label for each border node, accessible by workers in the next superstep.

This PEval differs from its counterpart given in [25] only in the following, marked with dotted underlines. VMap is applied to parallelize the initialization of status variables (Message Preamble). EMap parallelizes its recursion (Line 6) to conduct a round of BFS. It works on a set Δ of active vertices, which serves as the recursion queue for BFS. Function BFSRecur is passed to EMap as the update function f_E. For each *unvisited* neighbor v of the working vertex u (Line 9), BFSRecur overwrites v.root with u's CRoot (Line 10), and adds v to the recursion queue by returning $\{v\}$ (Line 11). During the process, EMap makes parallel visits to the neighboring vertices.

(2) IncEval. As shown in Algorithm 4, IncEval *incrementally* refines the partial result CC_i at F_i, based on messages (updates) from other subgraphs. IncEval (a) updates the label $L_i(v_r)$ of each CRoot v_r as the smallest of its descendants in the same connected component (Line 1); and (b) refines CC_i by merging CRoots $(u_r, v_r \in CC_i)$ with the same label, and sets their root to the remaining CRoot (Line 2). The messages are aggregated via min just like in PEval.

This IncEval differs from its counterpart of [25] in its VMap-based implementation of local message propagation. Here function UpdateRoot is passed to VMap as its update function f_V. For each vertex v that receives messages, UpdateRoot works in parallel to (a) find the CRoot v_r of v (Line 4–5), and (b) update the label of v_r by incorporating the incoming messages (Line 6).

(3) When no messages are generated, Assemble collects CRoots from all W_i's and counts the number of CRoots of distinct labels. □

Partial results. Under GC, PEval computes partial result $\mathcal{R}_i$ on the local subgraph F_i while IncEval refines $\mathcal{R}_i$ incrementally based on messages. In a distributed system like GRAPE, $\mathcal{R}_i$ can be cached in memory. However, in MiniGraph, it might exceed the memory capacity to cache all partial results. Thus MiniGraph opts to persist $\mathcal{R}_i$ together with its subgraph F_i. We embed $\mathcal{R}_i$ as the metadata of F_i, which will be discharged and loaded together with F_i.

Remark. GraphScope [20], an extension of GRAPE, supports VC and GC as two separate sets of programming interfaces. In contrast, MiniGraph enforces intra-subgraph VC parallelism to enrich inter-subgraph GC parallelism. This said, as will be seen shortly, one may readily cast a VC program into PIE+, *i.e.,* users may still choose to use either VC or GC that fits their applications and graphs the best.

Algorithm 5: PR under PIE+.

Input: subgraph $F_i = (V_i, E_i)$, a threshold ϵ.
Output: the rank of every v in V_i.

/* declare status variable: v.sink = 0 for each $v \in V_i$; */
Function PEval **(F_i):**
1 VMap (V_i, function (v) { v.rank := rand(); **return** $\emptyset$; });
2 EMap (V_i, Propagate); VMap (V_i, UpdateRank); **return** $\emptyset$;
Function IncEval **(F_i, M_i):**
3 VMap (M_i, function (m) { v.rank := m.rank; **return** $\emptyset$; });
4 VMap (V_i, function (v) { v.sink = 0; **return** $\emptyset$; });
5 EMap (V_i, Propagate); VMap (V_i, UpdateRank); **return** $\emptyset$;
6 **Procedure** Propagate (u, v):
7 v.sink := v.sink + u.rank/u.degree$^+$; **return** $\emptyset$;
8 **Procedure** UpdateRank (v):
9 v.rank := $d \cdot v$.sink + $(1 - d)$; **return** $\emptyset$;

4.2 Case Studies

We have shown how PIE+ parallelizes WCC (Example 4). Below we show how to program with PIE+ for three problems that fit VC, GC or both. The PIE+ programs are similar to their PIE counterparts [25], and hence we emphasize the use of EMap and VMap.

PageRank: from VC to PIE+. As remarked earlier, EMap and VMap together support full-fledged VC programming (see [57]). This makes it possible for PIE+ to program an arbitrary VC algorithm, by simply recasting it into EMap and VMap. We illustrate this with PageRank (PR [14]), a typical VC program.

PR takes as input a directed graph $G = (V, E)$ (*e.g.,* hyperlinks among Web pages) and a threshold ϵ, and outputs the ranking scores of all vertices in G. For each vertex v in V, its ranking score is:

$$v.\text{rank} = d \cdot \Sigma_{\{u \mid \langle u,v \rangle \in E\}} \frac{u.\text{rank}}{u.\text{degree}^+} + (1 - d), \qquad (1)$$

where d is a user-defined damping factor and $u.\text{degree}^+$ denotes the out-degree of u. This update function is applied iteratively to refine the ranking scores, until the Euclidean distance between the ranks in two consecutive iterations is below the predefined threshold ϵ.

As shown in Algorithm 5, we simply implement Equation 1 with EMap and VMap, and embed them in PEval and IncEval.

PEval *and* IncEval. For each vertex v in V_i of subgraph F_i, PEval (1) declares its status variable v.sink, initialized as 0 (Line 7); (2) initializes v.rank with a random float in (0, 1) by invoking rand() with VMap (Line 1); (3) propagates v.rank to each out-neighbor u, accumulating the scores in u.sink; and (4) updates v.rank by Equation 1 based on the score accumulate in v.sink (Line 2).

Steps (3) and (4) are parallelized via EMap and VMap, with update functions Propagate and UpdateRank, respectively. EMap executes Propagate for all vertices in parallel. Each call to Propagate performs rank propagation along an edge $\langle v, u \rangle$. It sends the source rank v.rank to u and calculates accumulated ranking scores in u.sink by Equation 1 (Line 7). Then VMap runs UpdateRank in parallel, to update the score of every vertex v based on v.sink (Line 9).

IncEval is similar to PEval except that it (1) starts with border nodes updated by messages (Line 3), and (2) resets v.sink for each v in V_i to 0 (Line 4). Both steps are parallelized with VMap.

Assemble is triggered as soon as the changes between two consecutive IncEval iterations are below threshold ϵ. It simply collects the ranking scores of all vertices, and returns the scores as output.

Remarks. Algorithm 5 is a representative example for converting a VC algorithm into a PIE+ program. It shows how to parallelize vertex-centric operations with EMap and VMap. In general, given a VC algorithm such as a GAS program of PowerGraph [30], we may convert it into a PIE+ program as follows: (1) declare an intermediate hashmap Π for caching incoming messages at all vertices; (2) recast Scatter with VMap to generate the outgoing message for each vertex; (3) recast Gather with EMap to perform the message passing via adjacent edges of each vertex, and caching/aggregating them in the corresponding receiver entries of Π; (4) recast Apply with VMap to update each vertex based on its own status and its aggregated messages in Π; (5) embed the implementation above in PEval and IncEval; and (6) specify Assemble based on the output.

Graph simulation. We next study an algorithm that is easy to write under GC, but is nontrivial under VC. Consider a graph pattern $Q = (V_Q, E_Q, L_Q)$, which is defined just like graphs (Section 2). Given a pattern $Q = (V_Q, E_Q, L_Q)$, a *match* of Q in graph $G = (V, E, L)$ via graph simulation, denoted by Sim, is a binary relation $R \subseteq V_Q \times V$ such that (1) for each pair $(u, v) \in R$, $L_Q(u) = L(v)$; and (2) for each pattern vertex $u \in V_Q$, there exists a vertex $v \in V$ such that (a) $(u, v) \in R$, and (b) for each pattern edge $\langle u, u' \rangle \in E_Q$, there is an edge $\langle v, v' \rangle \in E$ such that $(u', v') \in R$. If G matches Q, there exists a *unique maximum* relation [33], denoted as $Q(G)$; otherwise, $Q(G)$ is an empty set. It is in quadratic time to compute $Q(G)$ [33].

Outline. We show how PIE+ implements the algorithm of [33] for Sim, denoted as $\mathcal{A}_{\mathsf{sim}}$. Given a pattern Q and a graph G, $\mathcal{A}_{\mathsf{sim}}$ computes the unique maximum relation $Q(G)$. It maintains a set $\mathsf{sim}(u)$ for each pattern vertex $u \in V_Q$, initialized as the set of all vertices v in G that bear the same label as $L_Q(u)$; it then refines $\mathsf{sim}(u)$ iteratively by removing invalid candidates until a fixpoint is reached.

Under PIE+, $\mathcal{A}_{\mathsf{sim}}$ is a minor adaptation from the PIE program of [25]. It works as follows on every subgraph F_i. (1) It declares a Boolean variable $x(u, v)$ for each pattern vertex u in Q and each vertex v in F_i; flag $x(u, v)$ is set true if v is a potential match of u; it is reset to false when v is removed from $\mathsf{sim}(u)$. (2) PEval refines $\mathsf{sim}(u)$ for all $u \in V_Q$ and computes $Q(F_i)$ following [33]. At the end of PEval, each worker aggregates $x(u, v)$ into MessageStore by taking a conjunction in v's corresponding entry. (3) IncEval is the incremental simulation algorithm of [23], which treats message updates as edge deletions. It works on each status variable in the messages, propagates the changes to the affected area, and refines $\mathsf{sim}(u)$. At the end of each IncEval process, *changed* flags $x(u, v)$ of border nodes v are aggregated by W_p just like in PEval. (4) Assemble is triggered when no more messages are exchanged; it takes a union of $Q(F_i)$ for all i and returns the union as $Q(G)$.

Use of EMap and VMap. Algorithm $\mathcal{A}_{\mathsf{sim}}$ parallelizes edge/vertex-level operations with EMap and VMap. (1) During PEval initialization, VMap is used to assign the initial match set $\mathsf{sim}(u)$ for all $u \in V_Q$ in parallel. (2) Later in PEval, VMap parallelizes refinement of $\mathsf{sim}(u)$ for each u, during which EMap is used to check invalid matches of neighbors of u in parallel. (3) In IncEval, VMap parallelizes incremental processing of each "edge deletion".

Remarks. PR is a representative example for converting a GC algorithm into a PIE+ program. In general, the conversion is as follows: (1) start from its PIE program, which typically parallelizes an efficient sequential algorithm; (2) identify independent operations, *e.g.,* loops that iterate on an edge/vertex set, as commonly found in graph algorithms; and (3) replace these loops with an EMap or a VMap, passing in an update function that is functionally equivalent.

Single-source shortest path (SSSP**)**. We next present a PIE+ algorithm for a problem for which algorithms are known under both GC and VC. Consider a directed graph $G = (V, E, L)$, where edge label $L(e)$ is a positive number for $e \in E$. The length of a path $\langle u_0, u_1, \ldots, u_k \rangle$ in G is $\Sigma_{i=0}^{k-1} L(\langle u_i, u_{i+1} \rangle)$. For a pair (s, d) of vertices in V, $\mathsf{dist}(s, d)$ denotes the shortest distance from s to d. Given G and a source $s \in V$, SSSP is to compute $\mathsf{dist}(s, v)$ for all $v \in V$.

Outline. For subgraph F_i, we declare a variable $x(v)$ for all v in F_i, denoting $\mathsf{dist}(s, v)$. These status variable are initialized as ∞ except $x(s) = 0$. PEval implements the Dijkstra's algorithm [27], and computes $x(v)$ for all v along paths within F_i. MessageStore aggregates $x(v)$ of border nodes by taking min as aggregate function f_{aggr}. Then, IncEval follows the incremental SSSP algorithm in [54] upon receiving the updated $x(v)$ values as messages. It refines local $x(v)$ values iteratively, by recalculating shortest paths from border nodes v with updated $x(v)$. When no further updates can be made to any $x(v)$, Assemble aggregates $\mathsf{dist}(s, v)$ for all v in V.

Use of EMap. In both PEval and IncEval, a vertex v is marked *active* if its $x(v)$ is updated. All active vertices are cached in a min heap, sorted by $x(v)$. The algorithm iteratively (1) removes the minimum element v from the heap and marks it *inactive*; and (2) checks every neighbor u of v, and updates $x(u)$ with a smaller value if it exists. The PIE+ program employs EMap to parallelize accesses to v's neighbors, similar to BFSes in WCC (see Line 6 of Algorithm 3).

5 EXECUTION MODEL

In this section, we present the execution model of MiniGraph.

Workflow. Taking subgraphs $F_0, F_1, \ldots, F_{n-1}$ of graph G as input, MiniGraph executes a PIE+ program $\mathcal{A}$ in BSP supersteps (rounds). Each round iterates over all subgraphs: the first is a PEval round, followed by IncEval rounds, on each subgraph. A new IncEval round cannot start until the last round completes, and messages generated in the current round are pulled when the next (IncEval) round starts.

Within a round, unprocessed on-disk subgraphs are loaded one after another, while in-memory subgraphs are processed by concurrent workers. To process subgraph F_i, its virtual worker W_i is allocated p_i physical threads from available ones in ThreadPool by Scheduler; W_i then pulls messages generated in the last round, conducts computations on F_i, and aggregates new messages; it releases resources back to Scheduler before it is deactivated.

The scheduling problem. Scheduler has to make two decisions at runtime: (1) when to load and process a subgraph, and (2) how to allocate resources to maximize two-level parallelism. Making optimum decisions for these is, however, highly nontrivial.

A cost model. Given a PIE+ program $\mathcal{A}$, we train a cost function $C_{\mathcal{A}}$ to estimate the execution time of worker W_i on subgraph F_i. We adapt the cost function $C_{\mathcal{A}_{\mathsf{PIE}}}$ of [21] for PIE program $\mathcal{A}_{\mathsf{PIE}}$:

$$C_{\mathcal{A}_{\mathsf{PIE}}}(F_i) = \Sigma_{v \in F_i} h_{\mathcal{A}_{\mathsf{PIE}}}(\bar{x}_i(v)), \tag{2}$$

where for a vertex v in F_i, $h_{\mathcal{A}_{\mathsf{PIE}}}$ is a learnable polynomial regression model defined over a vector $\bar{x}_i(v)$ of *metric variables*. Here $\bar{x}_i(v)$

takes into account the average in/out-degree of all vertices in G, and several structural information of v, *e.g.,* v's in/out-degree in F_i and G, and the number of v's mirror across all subgraphs of G.

Following [21], we define $C_{\mathcal{A}}$ for a PIE+ program $\mathcal{A}$ as

$$C_{\mathcal{A}}(F_i, p_i) = \sum_{v \in F_i} [h^{\text{seq}}_{\mathcal{A}}(\bar{x}_i(v)) + \frac{h^{\text{para}}_{\mathcal{A}}(\bar{x}_i(v))}{\min\{p_i, \lfloor d_i \rfloor\}}], \tag{3}$$

where p_i denotes the number of allocated threads for worker W_i, d_i is the average degree of vertices in F_i, and $h^{\text{seq}}_{\mathcal{A}}$ and $h^{\text{para}}_{\mathcal{A}}$ are learnable models like $h_{\mathcal{A}_{\text{PIE}}}$. Intuitively, the cost of $\mathcal{A}$ is broken into $h^{\text{seq}}_{\mathcal{A}}$ for unparallelizable computations and $h^{\text{para}}_{\mathcal{A}}$ for parallelizable operations (those defined in EMap and VMap). When more cores p_i are allocated, $h^{\text{para}}_{\mathcal{A}}$ may get a linear speedup subject to maximum d_i.

We train $C_{\mathcal{A}}$ as a polynomial regression model with training samples from historic running logs, following [21]. We take stochastic gradient descent [12], using mean square error as the loss function.

Problem formulation. With $C_{\mathcal{A}}$, we model the scheduling problem as an optimization problem. Given subgraphs $F_0, F_1, \ldots, F_{n-1}$ of G and an m-core machine with memory size η, it is to find an optimal schedule $\mathcal{S} = (\bar{t}, \bar{p})$, where $t_i \in \bar{t}$ and $p_i \in \bar{p}$ denotes the start time and thread allocation of W_i for all i in $[0, n)$. Its objective function is

$$\arg\min_{\mathcal{S}} \max_{i \in [0,n)} \{t_i + C_{\mathcal{A}}(F_i, p_i)\}. \tag{4}$$

It is to minimize the *makespan* of $\mathcal{S}$, *i.e.,* the overall completion time of all workers. At any point, a *valid* schedule is subject to three constraints: (1) the consumed memory cannot exceed η; (2) the total thread allocation cannot exceed m; and (3) the start time t_i cannot be set before F_i is fully loaded into the memory, for all i in $[0, n)$. Note that the final constraint takes into account the I/O cost under the memory capacity η. It models the behavior of Loader (see Section 3), which loads fragments continuously as long as η is not exhausted.

Its decision problem, denoted by DSP, is to decide, given the input and a deadline B, whether there exists a valid schedule $\mathcal{S}$ with makespan at most B. The problem is intractable; it subsumes the NP-complete problem of *malleable parallel task scheduling* [44].

Theorem 1: DSP *is NP-complete.* □

Proof sketch: DSP is in NP since one can guess a schedule and check in PTIME whether it is valid and its makespan is at most B. We show that it is NP-complete by reduction from the set partition problem, which is known NP-complete [28] (see [6] for a proof). □

Scheduling strategy. Due to the intractability, Scheduler adopts a lightweight strategy. Offline for each subgraph F_i, it collects its size information and assigns F_i a number $\hat{p}_i$. Then at runtime, it loads pending subgraphs and launches new workers greedily, such that at least $\hat{p}_i$ threads are allocated to W_i. If idle threads exist with no available worker to launch, they are reallocated to active workers.

Intuitively, we strike a balance between inter-subgraph parallelism and intra-subgraph parallelism. It ensures that each subgraph is allocated at least $\hat{p}_i$ threads. Then whenever a set T of threads gets freed, we prioritize pending subgraphs F_i if $|T| \geq \hat{p}_i$. We set $\hat{p}_i$ heuristically to estimate the optimal allocation for worker W_i, given the CPU and memory constraint. This strategy satisfies $\hat{p}_i$ for W_i greedily and thus approximates the optimal schedule.

Tentative resource allocation. Scheduler allocates resources based on the subgraph size and the memory size η. It sets $\hat{p}_i = \lceil \frac{s(F_i)}{\eta} m \rceil$ for worker W_i, where $s(F_i)$ is the binary size of F_i. Intuitively, $\hat{p}_i$ indicates the *minimum* number of threads for W_i to process F_i, to strike a balance between computing and memory resources. Following *multi-resource scheduling* [31], all threads are allocated *before* the memory gets exhausted, prioritizing CPU utilization.

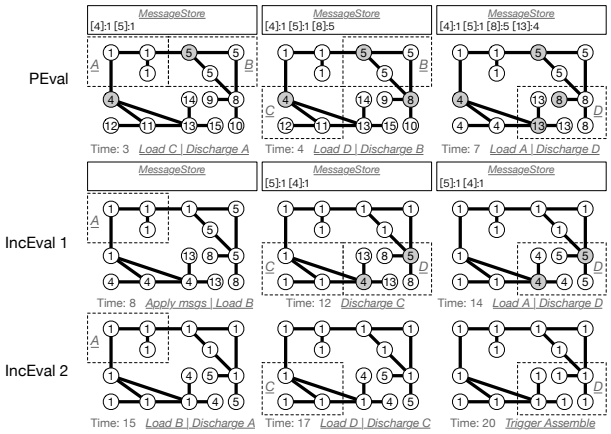

Figure 3: WCC on G with the two-level parallel execution model.

Greedy subgraph processing. At runtime, Scheduler keeps track of a list of pending subgraphs, sorted by their sizes. To select one for processing, it prioritizes the largest one whose tentative allocation can be satisfied. When Scheduler is triggered by an event that t threads are freed by a worker, it is to load the largest F_i with $\hat{p}_i \leq t$.

Intra-subgraph parallelism. When the unallocated threads cannot satisfy the tentative allocation of any pending subgraph, Scheduler allocates these free threads to active workers, one at a time, as it thrives to keep all CPU cores busy. It decides the receiving worker based on cost analysis. (1) With pending subgraphs, it estimates $\Delta_i = C_{\mathcal{A}}(F_i, p_i) - C_{\mathcal{A}}(F_i, p_i + 1)$ for all active workers, and selects W_j with the highest Δ_j, *i.e., W_j* gets the most speedup from the extra thread. (2) With no subgraph pending processing for the round, it selects W_j with the maximum $C_{\mathcal{A}}(F_j, p_j)$ to improve the straggler.

Such reallocations are temporary; whenever a new worker W_j becomes active, these available threads are retracted by Scheduler and reassigned to W_j to meet its demand of $\hat{p}_j$ threads.

Example 5: Continuing with Example 3, we compute WCC over G (Figure 1a) on a 4-core machine. Suppose that each subgraph takes 1 time unit to load/write, and each message passing takes 1 time unit. The tentative allocation assigns 2 threads to each worker. As shown in Figure 3, WCC passes all 32 message in 19 time units, leveraging both pipelined processing and two-level parallelism. □

6 IMPLEMENTATION AND OPTIMIZATION

In this section, we outline our implementation of MiniGraph and present its unique optimization strategies.

Implementation. MiniGraph is implemented in 12k+ lines of C++ code, based on the pipelined architecture of Figure 2. A thread is dedicated to Loader, which responds to read requests and loads subgraphs into memory, one at a time; similarly for Discharger. Both components perform synchronous I/O, and consume few CPU cycles. Evaluator maintains a thread pool for active workers, of size m on an m-core machine. Scheduler allocates threads to available

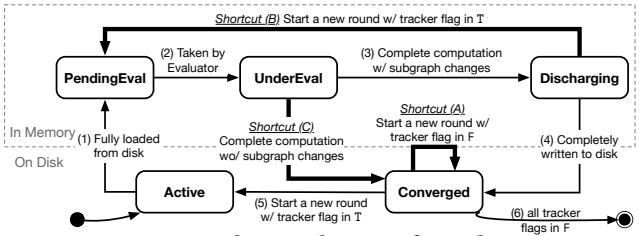

Figure 4: The state diagram of a worker.

cores. Moreover, Evaluator can move a thread from an active worker to another, without interrupting their executions and with negligible cost in light of shared memory. The dynamic thread reallocation is easy since EMap and VMap readily decompose computation on each subgraph into *independent* calls to (low-cost) update functions f_E and f_V. MiniGraph employs MessageStore as the central exchange point for messages. To make a low memory footprint and improve concurrency, it is implemented as an array; it incurs a lower space and time cost than a key-value store (*e.g.,* a hashmap).

Optimization. Recall Example 5. In Figure 3, Subgraph A is not updated in both IncEval steps, and its worker receives no messages (updates); thus it requires no further processing, and there is no need to even load Subgraph A. To reduce the unnecessary I/O for loading/discharging Subgraph A, MiniGraph employs (a) a list $\mathcal{M}$ of flags that helps track message exchanges among workers, and (b) a lightweight state machine for modeling the progress of each worker. Both $\mathcal{M}$ and state machine are maintained by StateManager.

Message tracking. StateManager builds a list $\mathcal{M}$ of flags, one for each worker to indicate whether the worker has any messages. It sets $\mathcal{M}[i]$ true if worker W_i has at least one pending update to pull from MessageStore. Otherwise, W_i requires no incremental work to be done, and thus IncEval can be safely skipped in the next round.

Example 6: Continuing with Example 5, the step-by-step WCC execution is shown in Figure 3. Before starting Step IncEval 1, the flags are `[F,T,T,T]` for Subgraph A, B, C and D, respectively. Note that Subgraph A receives no messages in this round, and hence its flag is F. Similarly, the flags are `[F,F,F,T]` for Step IncEval 2. □

Worker states and state transitions. We use a finite state machine to model the progress at each worker W_i, and flag $\mathcal{M}[i]$ to trigger state transitions of W_i. As shown in Figure 4, at any point, a worker is in one of the five states: Active, Converged, PendingEval, UnderEval, and Discharging. The first two indicate that the corresponding subgraph is on-disk, while the rest are in-memory states.

For a PEval or IncEval round, worker W_i traverses all five states. As shown in Figure 4, it starts from Active, indicating that W_i requires further computation (*e.g.,* with unconsumed updates). Then, (1) after its subgraph data F_i is loaded into the memory by Loader, W_i becomes PendingEval, meaning that W_i is ready to run and requests thread allocation; (2) W_i turns to UnderEval, after it is taken by Evaluator and under active computation; (3) when W_i concludes with changes made to F_i, its metadata (*e.g.,* status variables, partial results) and messages aggregated in MessageStore, W_i is set to Discharging; and (4) once F_i is fully persisted on disk, Discharger releases its memory space and sets W_i to Converged, indicating that it is done for the round. MiniGraph concludes the round when all workers get past UnderEval. If there are messages cached in MessageStore, MiniGraph (5) resets Converged workers back to Active, and starts a new round of (IncEval) computation. Otherwise, MiniGraph (6) calls Assemble to produce the final results.

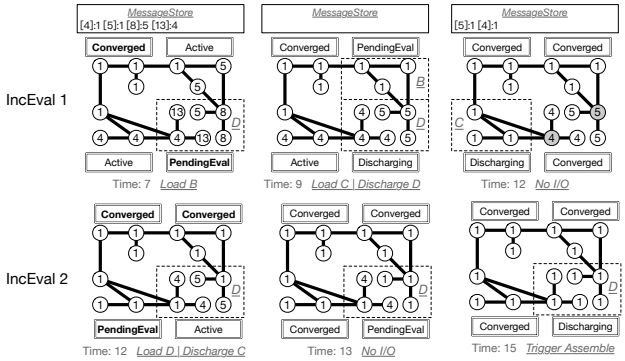

Figure 5: Optimized WCC execution on G with shortcuts.

Shortcuts in state transitions. Under certain conditions, some states in a round of computation can be skipped without affecting the correctness. That is, MiniGraph can take some "shortcuts" in state transitions, and reduce unnecessary computation and I/O. Below are example shortcuts identified by StateManager, marked as bold arrows in Figure 4. Consider worker W_i with its flag $\mathcal{M}[i]$.

Shortcut (A). To start of a round of IncEval computation, the state of W_i is typically reset to Active following transition (5). If $\mathcal{M}[i]$ = F, however, we may keep W_i in Converged state as it requires no further processing. That is, we can skip handling subgraph F_i in the round. This shortcut is frequently exploited when the input graph is, *e.g.,* not well-connected and F_i is "isolated".

Shortcut (B). MiniGraph starts a new round of IncEval as soon as all workers finish the current round (*i.e.,* get past UnderEval). If W_i is still in Discharging, *i.e.,* if its changed F_i is not yet fully persisted onto the disk, W_i is set to PendingEval directly, such that it starts the new round without going through the disk. This shortcut is exploited at the end of each round and substantially reduces I/O.

Shortcut (C). When W_i completes with no changes to F_i or its metadata, W_i skips Discharging and is set to Converged directly, avoiding redundant disk writes. This shortcut is effective for, *e.g.,* SSSP.

Example 7: Continuing with Example 5–6, we show execution of WCC in Figure 5 by exploiting shortcuts in state transitions (in bold state labels). PEval execution remains the same as in Figure 3.

The start of Step IncEval 1 (Time 7) sees two shortcuts: (1) worker A takes Shortcut (A) to skip computation entirely; and (2) worker D skips discharging/loading by taking Shortcut (B); it enters PendingEval directly for the next round of IncEval. Because of the two shortcuts, Step IncEval 1 takes 5 time units to complete (Time 7–12), as opposed to 7 time units (Time 7–14) in Example 5.

Similarly, we optimize Step IncEval 2. It takes 3 time units (Time 12–15), a 40% reduction from 5 units (Time 14–19) in Example 5. □

7 EXPERIMENTAL EVALUATION

Using real-life graphs, we evaluated MiniGraph for its (1) efficiency, (2) scalability and (3) performance versus multi-machine systems.

Experimental setup. We start with the settings.

Datasets. We used six real-life datasets of different types: road network, network topology, social graphs and Web graphs, as detailed in Table 2. Among these, `clueWeb` far exceeds the memory capacity of a single machine. We adopted an edge-cut partitioner [43] for

Name	Type	$\|V\|$	$\|E\|$	MaxDegree	Raw Data
roadNetCA [1]	road network	2M	2.7M	23	83MB
skitter [42]	network topology	1.6M	11M	35455	142MB
twitter [8, 40]	social network	41.6M	1.5B	3M	25GB
friendster [5]	social network	65.6M	1.8B	5124	30.14GB
web-sk [55]	Web	50M	1.9B	8.5M	32GB
clueWeb [55]	Web	1.7B	7.9B	6.4M	137GB

Table 2: Graph datasets.

these graphs. MiniGraph also works with other partitioners.

Baselines. We evaluated three out-of-core systems as baselines: GridGraph [76], GraphChi [41] and XStream [56]. GridGraph is the state-of-the-art, assuming an off-the-shelf hardware platform. We did not test Mosaic [47] since it requires an Intel Xeon Phi coprocessor, which has been discontinued since 2018 [51]. We also omitted in-memory systems (*e.g.,* [46, 53, 57, 71, 73]) since MiniGraph targets applications when the input graph cannot fit into the memory.

We tested two variants of MiniGraph: (1) $\text{MiniGraph}_{\text{Seq}}$, which exposes PIE as interface without EMap and VMap (Section 4.1). (2) $\text{MiniGraph}_{\text{NoShort}}$, which disables shortcuts (Section 6).

We also compared with GraphScope [20] and Gluon [17], which use multiple machines, not a single machine as MiniGraph.

Algorithms and queries. We implemented PIE+ programs (Section 4) for WCC, SSSP, PR and Sim. The first three are included in various benchmarks [7, 11]. For baselines, we used their out-of-box implementations for the first three. No baselines support Sim out-of-box. We implemented the VC-based Sim algorithm of [26] on GraphChi. However, the algorithm cannot be implemented on GridGraph or XStream without changing their internal working, because a necessary global storage is not supported by the APIs of either system.

For each input graph for SSSP, we randomly picked 10 vertices and used them as source vertices. For Sim, we randomly generated 20 query patterns, each of which has 6 vertices and 10 edges.

We deployed the single-machine systems on a workstation running Ubuntu Server 20.04 LTS, powered with an Intel Core i9-7900X CPU @3.30GHz and 64GB of DDR4-2666 memory. The CPU has a 13.75MB LLC, shared among 10 cores (20 hyperthreads).

Unless stated otherwise, we set n partitions as reported in Table 4 such that we have $\hat{p}_i = 4$ by default (see Section 5). We set a different n for PR (*s.t.* $\hat{p}_i = 10$), guided by our experiments with varying n (see [6] for details). Graphs are loaded from a 1TB WD Blue WDS100T2B0A SATA SSD, whose average sequential read throughput is 560MB/s. Each experiment was repeated 5 times; we report the average here. We report results for some algorithms on some graphs; the other results are consistent and are reported in [6].

Experimental results. We next report our findings.

Exp-1: Efficiency. We first evaluated the efficiency and I/O of MiniGraph versus out-of-core systems. Some experiments are conducted under a *memory budget*, *i.e.,* the ratio of the available memory to the size of the raw input. For instance, a 50% memory budget means that exactly *half* of the graph can be held in memory. We used Linux cgroups to enforce the memory budget, similar to [9].

SSSP. For SSSP over different graphs, Table 3 reports the number of supersteps, the volume of disk read traffic, I/O reduction from shortcuts, the average CPU utilization, the correlation coefficient r between real-time I/O and CPU usage, and the CPU cache hit rate. Table 3 only shows comparison with GridGraph, the best performing baseline. Table 4 shows the performance of all the systems.

Dataset	Metric	SSSP		WCC		PR	
		MiniGraph	GridGraph	MiniGraph	GridGraph	MiniGraph	GridGraph
friendster	# Supersteps	**8**	32	**6**	21	8	10
	Disk Read (GB)	**78**	115.1	**74**	135	**107**	160
	Shortcut I/O (GB)	**-12**	N/A	**-12**	N/A	**-10.4**	N/A
	Avg. CPU Util.	**33.74%**	4.45%	**48.2%**	6.83%	**68.46%**	62.38%
	I/O-Compute Corr.	**0.095**	-0.113	**0.163**	-0.202	**0.185**	-0.156
	Cache Hits	**45.33%**	9.59%	**48.25%**	12.04%	**34.8%**	**36.2%**
web-sk	# Supersteps	**10**	63	**9**	120	15	20
	Disk Read (GB)	**112.5**	232	**81.9**	367	**87**	232
	Shortcut I/O (GB)	**-30.9**	N/A	**-6.1**	N/A	**-20.9**	N/A
	Avg. CPU Util.	**15.76%**	5.83%	**25.04%**	5.16%	42%	**42%**
	I/O-Compute Corr.	**0.008**	0.003	**0.013**	0.009	**0.082**	-0.039
	Cache Hits	**50.89%**	6.37%	**37.42%**	11.63%	**50.22%**	46.04%

Table 3: Runtime statistics for SSSP, WCC and PR.

(1) MiniGraph performs the best over all out-of-core workloads, *i.e.,* input graphs that exceed the memory capacity (budget). With a 50% memory budget on friendster, on average MiniGraph outperforms GridGraph, GraphChi and XStream by 1.45×, 2.7× and 15.2×, respectively. It is 2.8×, 3.5× and 28.9× faster on web-sk.

The improvement of MiniGraph on web-sk is larger than on friendster, since web-sk is sparser and has a larger diameter. As remarked earlier, the VC model of the baselines supports within-neighborhood operations only, and thus requires more supersteps to converge on graphs with larger diameters. GridGraph, for instance, takes 32 supersteps on friendster and 63 on web-sk. In contrast, MiniGraph supports beyond-neighborhood computations via its hybrid parallel model. It takes 8 supersteps on friendster and 10 on web-sk. This justifies the need for GC and two-level parallelism.

(2) MiniGraph also substantially reduces disk I/O (Table 3). Compared to GridGraph, the best-performing baseline, it generates 32.3% and 51.6% less disk read traffic on friendster and web-sk, respectively. More specifically, (a) shortcuts (Section 6) account for 32.3% and 25.8% of the I/O reduction on friendster and web-sk, respectively. (b) The rest of I/O reduction roots in the reduced supersteps.

(3) The average CPU utilization of MiniGraph is 29.3% (resp. 9.9%) higher than GridGraph on friendster (resp. web-sk). GridGraph exhibits negative correlations ($r < -0.1$) between I/O and CPU usage, indicating that CPU may starve when the system is busy at loading data. In contrast, it is $0 < r < 0.1$ for MiniGraph; that is, its I/O does not block computations. These justify the pipelined architecture.

(4) MiniGraph has a much better CPU cache locality than GridGraph. It achieves a 45% cache hit rate on friendster and 51% on web-sk, while it is 10% for GridGraph at best (Table 3). This is because MiniGraph supports inter-subgraph parallelism, while VC systems (*e.g.,* GridGraph) frequently access all neighbors of each vertex, which inevitably incurs random reads across the entire graph.

(5) Over large clueWeb, MiniGraph performs substantially better than all the baselines. With a 47% memory budget, it outperforms GridGraph by 4.59×. When the memory budget is at 10%, it takes 1.63 hours, while no baseline completes within 5 hours.

MiniGraph underperforms prior systems in two cases over small graphs that can fit entirely into the memory. On skitter, *e.g.,* GridGraph takes 0.67× of the time of MiniGraph. This is because MiniGraph takes longer to initialize auxiliary data structures when it starts. Nonetheless, the margin is small (a 0.18s difference); for larger graphs, it is amortized by the I/O and computational costs.

(6) MiniGraph also performs substantially better than its variants. We defer a detailed discussion to the case of WCC below.

WCC. As shown in Tables 3-4, MiniGraph beats all the baselines for

Data	Memory Budget	#Partitions (PR/Others)	SSSP				WCC				PR			
			MiniGraph	GraphChi	GridGraph	XStream	MiniGraph	GraphChi	GridGraph	XStream	MiniGraph	GraphChi	GridGraph	XStream
roadNetCA	100%	1/1	8.66	22.5 (2.6×)	10.55 (1.2×)	**2 (0.2×)**	**2.76**	17.2 (6×)	18.22 (6.6×)	2.93 (1.1×)	**0.25**	0.91 (3.5×)	0.71 (2.7×)	2.34 (2.6×)
skitter	100%	1/1	0.53	41.64 (78.5×)	**0.35 (0.67×)**	0.69 (1.3×)	**0.16**	18.43 (115.2×)	0.33 (2.1×)	0.59 (3.9×)	**0.27**	1.27 (4.7×)	0.82 (3.0×)	0.98 (3.6×)
twitter	50% (12.5GB)	4/10	**150.8**	802.8(5.3×)	195.4(1.29×)	2365(15.6×)	**159.5**	594.8(3.7×)	186(1.2×)	1983(12.4×)	**224.2**	782.1(3.5×)	371.3(1.7×)	2183(9.7×)
friendster	50% (15.07GB)	4/10	**201.8**	535(2.7×)	293.1(1.45×)	3061(15.2×)	**171.8**	1636(9.5×)	204.7(1.2×)	2037(11.8×)	**190.104**	450.7(1.9×)	485.3(1.9×)	2685(11.3×)
web-sk	50% (16GB)	4/10	**326.4**	1140(3.5×)	917.9(2.8×)	9437 (28.9×)	**172**	620.1(3.6×)	704.6(4.1×)	4056(23.5×)	**248.3**	2288(9.2×)	395(1.6×)	2903(11.7×)
clueWeb	47% (64GB)	4/10	**2514**	/	11534 (4.59×)	/	**2742**	/	11665 (4.25×)	/	**2022**	/	3803(2.1×)	/
	10% (13.7GB)	20/50	**5871**	/	/	/	**7486**	/	/	/	**2979**	/	/	/

Table 4: Execution time for SSSP, WCC and PR (in seconds). "/" denotes that the experiment could not finish within 5 hours.

WCC over all graphs. (1) MiniGraph is up to 9.5×, 4.25× and 13.4× faster than GraphChi, GridGraph and XStream, respectively. (2) It takes only few supersteps (7.5%) and a fraction of disk read (28.9%) of GridGraph; it also has better average CPU utilization (+41.4%) and cache locality (+36.2%). (3) With 13.7GB memory, MiniGraph is the only system that works within 5 hours on web-sk. (4) MiniGraph generates 45.2% (resp. 77.8%) less disk read traffic on friendster (resp. web-sk), with 19.7% (resp. 2.2%) reductions from shortcuts.

MiniGraph also consistently outperforms its variants. As shown in Figure 6a, (a) It speeds up $\text{MiniGraph}_{\text{Seq}}$ by 61.0% and 78.1% on friendster and web-sk, respectively. This shows the benefit of its hybrid model that exploits intra-subgraph parallelism to improve multi-core parallelism. The hybrid model works better on denser graphs, which often allow a higher inherent intra-subgraph parallelism, to which EMap and VMap are more effective. (b) MiniGraph beats $\text{MiniGraph}_{\text{NoShort}}$ by 1.18× on average. This shows the effectiveness of the shortcut optimization in reducing I/O (Section 6).

Figure 6b shows the disk I/O and CPU utilization of MiniGraph and GridGraph over clueWeb. It verifies that MiniGraph overlaps I/O and CPU operations, and justifies its pipelined architecture.

PR. As reported in Table 4, (1) MiniGraph is 1.6–3.0× faster than GridGraph over all graphs, the best-performing baseline, although PR fits its VC model. (2) On friendster (resp. web-sk), MiniGraph incurs 33.1% (resp. 45.6%) less disk read traffic than GridGraph, with 19.6% (resp. 28.6%) reductions from shortcuts. These are higher than SSSP and WCC, since we use larger fragments in PR.

Sim. As shown in Figure 6c for Sim on friendster and web-sk, (1) on average MiniGraph beats GraphChi by 2.2× and 1.6×, and reduces I/O traffic by 81% and 77.4%, respectively. One reason is that a much more efficient algorithm for Sim can be supported by its hybrid model (see Section 4.2). Its complexity is $O((|E|+|V|)(|E_Q|+|V_Q|))$, where $|E|$ and $|V|$ (resp. $|E_Q|$ and $|V_Q|$) denote the size of edges and vertices of G (resp. the query pattern Q), respectively. In contrast, GraphChi can only use the Sim algorithm [26] under VC that takes $O(|E|^2(|V_Q|+|E_Q|))$ time. This further justifies the need for supporting GC. (2) Over friendster, the shortcut reduction (see Section 6) further reduces the execution time by 51%. This is because on a dense graph like friendster, Sim easily reaches a local fixpoint within a subgraph and yields chances for shortcuts.

HDD vs. SSD. We also tested the impact of using HDD as the secondary storage. When replacing SSD with a 3.6TB Seagate HDD, the average read throughput drops from 560MB/s to 125MB/s, and all the systems get slower, as expected. Nonetheless, as shown in Figure 6d, MiniGraph is less sensitive to the switch. On friendster, *e.g.,* it is slowed by 2.6×, while it is 3.3× and 2.9× for GridGraph and GraphChi, respectively. This is because (a) MiniGraph incurs less I/O traffic (see Table 3), and (b) it issues a small number of bulk I/O requests, which works well with HDD that has a high seek cost.

Exp-2: Scalability. Under 50% memory budget, we evaluated the scalability of MiniGraph with (1) the size $|G|$ of graphs G, and (2) the number m of CPU cores. We also tested the impact of (3) thread allocation p_i, and (4) the number n of partitions. We report the results of WCC and PR; the results of SSSP and Sim are consistent.

Varying $|G|$. We sampled graphs G from large clueWeb using Edge Sampling [35], with a scale factor δ that controls the fraction of edges to be sampled. As shown in Figure 6e when varying δ from 0.4 to 1.0 for WCC, (1) MiniGraph scales well with $|G|$. It takes 2.3× longer, while it is 2.6× for GridGraph. (2) MiniGraph also scales better than its variants. $\text{MiniGraph}_{\text{Seq}}$ and $\text{MiniGraph}_{\text{NoShort}}$ increase 3.5× and 3.16× when δ varies from 0.4 to 1.0. These further verify the effectiveness of our hybrid parallel model and optimization strategies. (3) When $|G|$ grows 2.5×, MiniGraph incurs only 2.29× I/O traffic, due to the shortcut optimizations.

Varying m. Varying the number m of cores from 4 to 20, we ran WCC and PR over web-sk. As shown in Figure 6f, (1) MiniGraph scales sub-linearly with m. (2) It scales better than GridGraph, which does not improve much (up to +4.3%) when m varies from 8 to 20. This is because GridGraph becomes I/O-bound when $m \geq 8$, which echoes with our findings in Figure 6b. (3) It also scales better than $\text{MiniGraph}_{\text{Seq}}$, which barely improves when $m \geq 4$ for the lack of intra-subgraph parallelism. These further justify the need for a hybrid parallel model. The results over friendster are consistent [6].

Varying p_i. We also tested the impact of p_i, the number of threads allocated to processing a subgraph. Over friendster and web-sk, Figure 6g reports how WCC works with varying p_i. For each graph partitioning, we mark its tentative allocation $\hat{p}_i$ (Section 5) with colored points. As shown there, $\hat{p}_i$ strikes a balance between the two levels of parallelism and improves the overall multi-core parallelism, by selecting a near-optimal value for p_i based on n and G.

Varying n. The number n of partitions impacts the inter-subgraph parallelism of MiniGraph. Varying n from 2 to 64 on web-sk, Figure 6h shows its impact on WCC and PR. (1) For VC-based PR, its optimal n is 4. This setting minimizes fragmentation while keeping the pipeline working. (2) $\text{MiniGraph}_{\text{Seq}}$ is very slow under a small n, as its CPU usage is limited by the low inter-subgraph parallelism. (3) For GC-based WCC, the optimal n is 16. Finding this optimum value requires a careful cost analysis, which we leave as future work.

Exp-3: Single-machine vs. multi-machine. We also evaluated the capacity of MiniGraph for graph analytics with a single machine versus multi-machine systems GraphScope and Gluon. To make a uniform testing environment, we deployed them in the cloud.

Execution time. Figure 7a reports the performance of the systems for Sim and PR over friendster. (1) For Sim, we used 8-vCPU 64GB-memory instances for all three systems since GraphScope and

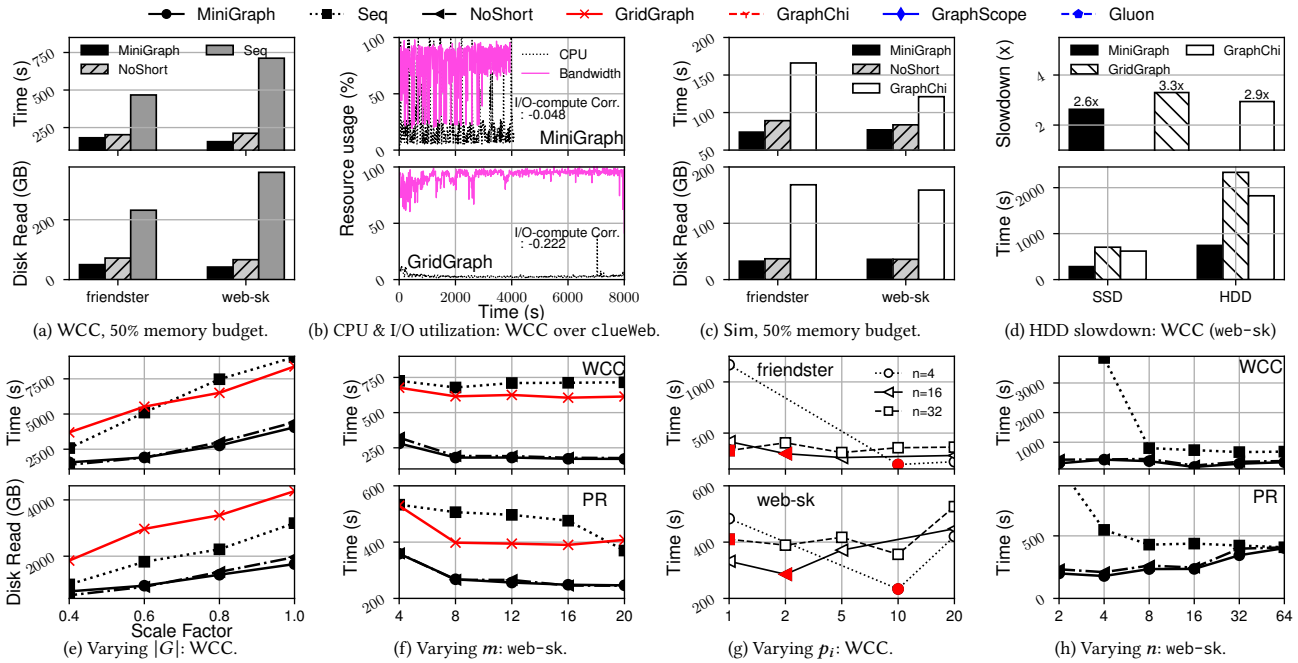

(a) WCC, 50% memory budget. (b) CPU & I/O utilization: WCC over `clueWeb`. (c) Sim, 50% memory budget. (d) HDD slowdown: WCC (`web-sk`)

(e) Varying $|G|$: WCC. (f) Varying m: `web-sk`. (g) Varying p_i: WCC. (h) Varying n: `web-sk`.

Figure 6: Efficiency and scalability of MiniGraph.

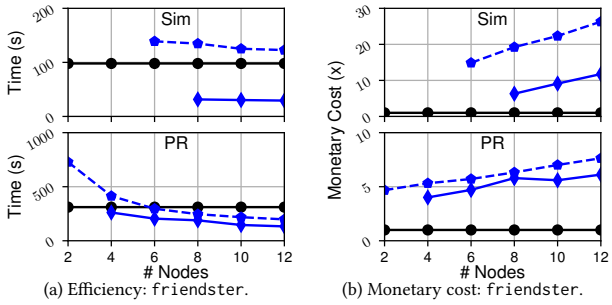

(a) Efficiency: `friendster`. (b) Monetary cost: `friendster`.

Figure 7: MiniGraph vs. multi-machine systems.

Gluon require more working memory. Gluon (resp. GraphScope) runs out-of-memory with fewer than 6 (resp. 8) nodes. MiniGraph, using a single instance, outperforms Gluon with up to 12 nodes by 29.3–46.3%. This further justifies the need for GC. While GraphScope takes less computation time, it requires an additional 200+s for preprocessing, which is not counted in Figure 7a. (2) For PR, MiniGraph runs on a single 8-vCPU 32GB-memory instance. Gluon uses a varying number of instances of the same configuration. GraphScope uses multiple 8-vCPU 64GB-memory instances, because it requires more than 32 GB in all cases of the experiment. Yet it still runs out-of-memory with 2 nodes. We find that MiniGraph performs comparably to a 4-node (resp. 6-node) deployment of GraphScope (resp. Gluon), and beats Gluon with fewer than 4 nodes.

Cost effectiveness. Figure 7b depicts the relative monetary cost of multi-machine systems for running Sim and PR over `friendster`, taking the cloud spending of MiniGraph as baseline. (1) While Gluon and GraphScope get faster with more nodes, they spend more. This echoes the observation of [49] that multi-machine parallelism is not always cost-effective. (2) GraphScope (resp. Gluon) pays at least 5.3× (resp. 13.9×) more than MiniGraph for Sim, and costs 3.0× (resp. 3.7×) more for PR. This further justifies the need for a single-machine system to save cost for small companies.

Summary. We find the following. (1) With the pipelined architecture and two-level parallelism, MiniGraph consistently outperforms the prior single-machine systems under all out-of-core workloads. It is up to 4.6×, 9.5× and 28.9× faster than GridGraph, GraphChi and XStream, respectively. (2) Under BSP, it requires only a fraction of supersteps (<29%) and disk read traffic (<53.3%) of GridGraph for SSSP and WCC. (3) It improves the CPU utlization of GridGraph, the best-performing baseline, by up to 41.4%. (4) It scales well with graphs and the number of CPU cores. With 13.7 GB of working memory, it runs all the algorithms on `clueWeb` within 2.08 hours, while no baseline finishes in 5 hours. (5) MiniGraph incurs less performance degradation when switching from SSD to HDD. (6) Its shortcut optimization is effective in reducing the I/O cost, especially on dense graphs. (7) Its two-level execution model balances inter-subgraph and intra-subgraph parallelism. (8) MiniGraph works better than Gluon with 12 machines on Sim, and saves the monetary cost of multi-machine systems from 3.0× to 13.9×.

8 CONCLUSION

The novelty of MiniGraph consists of (1) a pipelined architecture to overlap I/O and CPU operations, (2) the first out-of-core system that supports both GC and VC, (3) a two-level execution model to explore inter-subgraph parallelism and intra-subgraph parallelism, and (4) unique optimization opportunities to further reduce I/O. Our experimental study has verified that with a single machine, MiniGraph performs better than some 12-machine parallel systems.

One topic for future work is to extend the architecture of MiniGraph by incorporating GPU and FPGA. We have only considered CPU as a "lowest common denominator" of single-machine systems. When GPU and FGPA are available, we need to revise our workload assignment and graph partitioning strategies. Another topic is to support (adaptive) asynchronous parallel models [22].

REFERENCES

[1] 2010. Traffic dataset. http://www.dis.uniroma1.it/challenge9/download.shtml
[2] 2014. Timely Dataflow. https://github.com/frankmcsherry/timely-dataflow/
[3] 2015. COST. https://github.com/frankmcsherry/COST/
[4] 2020. GraphScope. https://graphscope.io/
[5] 2022. Friendster dataset. https://snap.stanford.edu/data/com-Friendster.html
[6] 2022. Full version. https://shuhaoliu.github.io/assets/papers/minigraph-full.pdf
[7] 2022. Graph500 benchmark specifications. https://graph500.org/?page_id=12#sec-3
[8] 2022. Twitter dataset. http://socialcomputing.asu.edu/datasets/Twitter
[9] Zhiyuan Ai, Mingxing Zhang, Yongwei Wu, Xuehai Qian, Kang Chen, and Weimin Zheng. 2017. Squeezing out all the value of loaded data: An out-of-core graph processing system with reduced disk I/O. In *USENIX ATC*. 125–137.
[10] Konstantin Andreev and Harald Racke. 2006. Balanced graph partitioning. *Theory of Computing Systems* 39, 6 (2006), 929–939.
[11] Scott Beamer. 2016. *Understanding and improving graph algorithm performance*. Ph.D. Dissertation. EECS Department, University of California, Berkeley.
[12] Christopher M Bishop and Nasser M Nasrabadi. 2006. *Pattern recognition and machine learning*. Vol. 4. Springer.
[13] Florian Bourse, Marc Lelarge, and Milan Vojnovic. 2014. Balanced graph edge partition. In *SIGKDD*. 1456–1465.
[14] Sergey Brin and Lawrence Page. 2012. The anatomy of a large-scale hypertextual Web search engine. *Computer Networks* 56, 18 (2012), 3825–3833.
[15] Hongzhi Chen, Changji Li, Chenguang Zheng, Chenghuan Huang, Juncheng Fang, James Cheng, and Jian Zhang. 2022. G-Tran: A high performance distributed graph database with a decentralized architecture. *PVLDB* 15, 11 (2022), 2545–2558.
[16] Joana MF da Trindade, Konstantinos Karanasos, Carlo Curino, Samuel Madden, and Julian Shun. 2020. Kaskade: Graph views for efficient graph analytics. In *ICDE*.
[17] Roshan Dathathri, Gurbinder Gill, Loc Hoang, Hoang-Vu Dang, Alex Brooks, Nikoli Dryden, Marc Snir, and Keshav Pingali. 2018. Gluon: A Communication-Optimizing Substrate for Distributed Heterogeneous Graph Analytics. In *PLDI*.
[18] Jing Fan, Adalbert Gerald Soosai Raj, and Jignesh M Patel. 2015. The Case Against Specialized Graph Analytics Engines. In *CIDR*.
[19] Wenfei Fan. 2022. Big Graphs: Challenges and Opportunities. *PVLDB* 15, 12 (2022), 3782–3797.
[20] Wenfei Fan, Tao He, Longbin Lai, Xue Li, Yong Li, Zhao Li, Zhengping Qian, Chao Tian, Lei Wang, Jingbo Xu, Youyang Yao, Qiang Yin, Wenyuan Yu, Kai Zeng, Kun Zhao, Jingren Zhou, Diwen Zhu, and Rong Zhu. 2021. GraphScope: A Unified Engine For Big Graph Processing. *PVLDB* 14, 12 (2021), 2879–2892.
[21] Wenfei Fan, Ruochun Jin, Muyang Liu, Ping Lu, Xiaojian Luo, Ruiqi Xu, Qiang Yin, Wenyuan Yu, and Jingren Zhou. 2020. Application Driven Graph Partitioning. In *SIGMOD*. ACM, 1765–1779.
[22] Wenfei Fan, Ping Lu, Wenyuan Yu, Jingbo Xu, Qiang Yin, Xiaojian Luo, Jingren Zhou, and Ruochun Jin. 2020. Adaptive Asynchronous Parallelization of Graph Algorithms. *ACM Trans. Database Syst.* 45, 2 (2020), 6:1–6:45.
[23] Wenfei Fan, Xin Wang, and Yinghui Wu. 2013. Incremental graph pattern matching. *ACM Trans. Database Syst.* 38, 3 (2013), 18.
[24] Wenfei Fan, Jingbo Xu, Yinghui Wu, Wenyuan Yu, Jiaxin Jiang, Bohan Zhang, Zeyu Zheng, Yang Cao, and Chao Tian. 2017. Parallelizing Sequential Graph Computations. In *SIGMOD*. ACM, 495–510.
[25] Wenfei Fan, Wenyuan Yu, Jingbo Xu, Jingren Zhou, XiaoJian Luo, Qiang Yin, Ping Lu, Yang Cao, and Ruiqi Xu. 2018. Parallelizing Sequential Graph Computations. *ACM Trans. Database Syst.* 43, 18 (2018).
[26] Arash Fard, M. Usman Nisar, Lakshmish Ramaswamy, John A. Miller, and Matthew Saltz. 2013. A distributed vertex-centric approach for pattern matching in massive graphs. In *IEEE BigData*. IEEE.
[27] Michael L Fredman and Robert Endre Tarjan. 1987. Fibonacci heaps and their uses in improved network optimization algorithms. *JACM* 34, 3 (1987), 596–615.
[28] Michael Garey and David Johnson. 1979. *Computers and Intractability: A Guide to the Theory of NP-Completeness*. W. H. Freeman and Company.
[29] Gurbinder Gill, Roshan Dathathri, Loc Hoang, Ramesh Peri, and Keshav Pingali. 2020. Single Machine Graph Analytics on Massive Datasets Using Intel Optane DC Persistent Memory. *PVLDB* 13, 8 (2020), 1304–1318.
[30] Joseph E. Gonzalez, Yucheng Low, Haijie Gu, Danny Bickson, and Carlos Guestrin. 2012. PowerGraph: Distributed Graph-Parallel Computation on Natural Graphs. In *USENIX*.
[31] Robert Grandl, Mosharaf Chowdhury, Aditya Akella, and Ganesh Ananthanarayanan. 2016. Altruistic Scheduling in Multi-Resource Clusters. In *OSDI*. 65–80.
[32] Minyang Han and Khuzaima Daudjee. 2015. Giraph Unchained: Barrierless Asynchronous Parallel Execution in Pregel-like Graph Processing Systems. *PVLDB* 8, 9 (2015), 950–961.
[33] Monika Rauch Henzinger, Thomas A. Henzinger, and Peter W. Kopke. 1995. Computing Simulations on Finite and Infinite Graphs. In *Annual Symposium on Foundations of Computer Science (FOCS)*. IEEE, 453–462.
[34] John E. Hopcroft and Robert Endre Tarjan. 1973. Efficient Algorithms for Graph Manipulation [H] (Algorithm 447). *CACM* (1973), 372–378.
[35] Pili Hu and Wing Cheong Lau. 2013. A survey and taxonomy of graph sampling. *arXiv preprint arXiv:1308.5865* (2013).
[36] Alekh Jindal, Samuel Madden, Malú Castellanos, and Meichun Hsu. 2015. Graph analytics using vertica relational database. In *IEEE Big Data*.
[37] Alekh Jindal, Praynaa Rawlani, Eugene Wu, Samuel Madden, Amol Deshpande, and Mike Stonebraker. 2014. Vertexica: Your relational friend for graph analytics! *PVLDB* 7, 13 (2014), 1669–1672.
[38] George Karypis and Vipin Kumar. 1998. Multilevelk-Way Partitioning Scheme for Irregular Graphs. *JPDC* 48, 1 (1998), 96–129.
[39] Mijung Kim and K Selçuk Candan. 2012. SBV-Cut: Vertex-cut based graph partitioning using structural balance vertices. *Data & Knowledge Engineering* 72 (2012), 285–303.
[40] Haewoon Kwak, Changhyun Lee, Hosung Park, and Sue Moon. 2010. What is Twitter, a social network or a news media?. In *WWW*.
[41] Aapo Kyrola, Guy E. Blelloch, and Carlos Guestrin. 2012. GraphChi: Large-scale graph computation on just a PC. In *OSDI*.
[42] Jure Leskovec, Jon M. Kleinberg, and Christos Faloutsos. 2005. Graphs over time: densification laws, shrinking diameters and possible explanations. In *SIGKDD*. ACM, 177–187.
[43] Yifan Li. 2017. *Edge partitioning of large graphs*. Ph.D. Dissertation. Université Pierre et Marie Curie-Paris VI.
[44] Walter T Ludwig. 1995. *Algorithms for Scheduling Malleable and Nonmalleable Parallel Tasks*. Ph.D. Dissertation. Department of Computer Sciences, University of Wisconsin-Madison.
[45] Hongbin Ma, Bin Shao, Yanghua Xiao, Liang Jeff Chen, and Haixun Wang. 2016. G-SQL: Fast query processing via graph exploration. *PVLDB* 9, 12 (2016), 900–911.
[46] Lingxiao Ma, Zhi Yang, Han Chen, Jilong Xue, and Yafei Dai. 2017. Garaph: Efficient GPU-accelerated Graph Processing on a Single Machine with Balanced Replication. In *USENIX ATC*. 195–207.
[47] Steffen Maass, Changwoo Min, Sanidhya Kashyap, Woon-Hak Kang, Mohan Kumar, and Taesoo Kim. 2017. Mosaic: Processing a Trillion-Edge Graph on a Single Machine. In *EuroSys*. ACM.
[48] Grzegorz Malewicz, Matthew H. Austern, Aart J. C. Bik, James C. Dehnert, Ilan Horn, Naty Leiser, and Grzegorz Czajkowski. 2010. Pregel: A system for large-scale graph processing. In *SIGMOD*. 135–146.
[49] Frank McSherry, Michael Isard, and Derek Gordon Murray. 2015. Scalability! But at what COST?. In *HotOS*.
[50] Robin Milner. 1989. *Communication and Concurrency*. Prentice Hall.
[51] Timothy Prickett Morgan. 2018. The End of Xeon Phi - It's Xeon and Maybe GPUs From Here. https://www.nextplatform.com/2018/07/27/end-of-the-line-for-xeon-phi-its-all-xeon-from-here/.
[52] Derek G Murray, Frank McSherry, Rebecca Isaacs, Michael Isard, Paul Barham, and Martín Abadi. 2013. Naiad: A timely dataflow system. In *SOSP*. ACM, 439–455.
[53] Donald Nguyen, Andrew Lenharth, and Keshav Pingali. 2013. A lightweight infrastructure for graph analytics. In *SOSP*. ACM, 456–471.
[54] G. Ramalingam and Thomas Reps. 1996. An incremental algorithm for a generalization of the shortest-path problem. *J. Algorithms* 21, 2 (1996), 267–305.
[55] Ryan A. Rossi and Nesreen K. Ahmed. 2015. The Network Data Repository with Interactive Graph Analytics and Visualization. In *AAAI*. 4292–4293.
[56] Amitabha Roy, Ivo Mihailovic, and Willy Zwaenepoel. 2013. X-stream: Edge-centric graph processing using streaming partitions. In *SOSP*. ACM, 472–488.
[57] Julian Shun and Guy E. Blelloch. 2013. Ligra: A lightweight graph processing framework for shared memory. In *SIGPLAN*. ACM, 135–146.
[58] Ryan Smith. 2022. Intel To Wind Down Optane Memory Business - 3D XPoint Storage Tech Reaches Its End. https://www.anandtech.com/show/17515/intel-to-wind-down-optane-memory-business.
[59] Benjamin A Steer, Alhamza Alnaimi, Marco ABFG Lotz, Felix Cuadrado, Luis M Vaquero, and Joan Varvenne. 2017. Cytosm: Declarative property graph queries without data migration. In *GRADES*.
[60] Stergios Stergiou, Dipen Rughwani, and Kostas Tsioutsiouliklis. 2018. Shortcutting label propagation for distributed connected components. In *WSDM*.
[61] Wen Sun, Achille Fokoue, Kavitha Srinivas, Anastasios Kementsietsidis, Gang Hu, and Guotong Xie. 2015. SQLGRAPH: An efficient relational-based property graph store. In *SIGMOD*. 1887–1901.
[62] Nilothpal Talukder and Mohammed J. Zaki. 2016. A distributed approach for graph mining in massive networks. *Data Mining and Knowledge Discovery* 30, 5 (2016), 1024–1052.
[63] Yuanyuan Tian, Andrey Balmin, Severin Andreas Corsten, Shirish Tatikonda, and John McPherson. 2013. From" think like a vertex" to" think like a graph". *PVLDB* 7, 3 (2013), 193–204.
[64] Leslie G. Valiant. 1990. A Bridging Model for Parallel Computation. *CACM* 33, 8 (1990), 103–111.
[65] Keval Vora, Guoqing Xu, and Rajiv Gupta. 2016. Load the Edges You Need: A Generic I/O Optimization for Disk-based Graph Processing. In *USENIX ATC*. 507–522.

[66] Guozhang Wang, Wenlei Xie, Alan J. Demers, and Johannes Gehrke. 2013. Asynchronous Large-Scale Graph Processing Made Easy. In *CIDR*.
[67] Chenning Xie, Rong Chen, Haibing Guan, Binyu Zang, and Haibo Chen. 2015. SYNC or ASYNC: Time to fuse for distributed graph-parallel computation. In *PPOPP*.
[68] Xianghao Xu, Fang Wang, Hong Jiang, Yongli Cheng, Dan Feng, and Yongxuan Zhang. 2020. A Hybrid Update Strategy for I/O-Efficient Out-of-Core Graph Processing. *TPDS* 31, 8 (2020), 1767–1782.
[69] Da Yan, James Cheng, Yi Lu, and Wilfred Ng. 2014. Blogel: A Block-Centric Framework for Distributed Computation on Real-World Graphs. *PVLDB* 7, 14 (2014), 1981–1992.
[70] Da Yan, James Cheng, Kai Xing, Yi Lu, Wilfred Ng, and Yingyi Bu. 2014. Pregel Algorithms for Graph Connectivity Problems with Performance Guarantees. *PVLDB* 7, 14 (2014), 1821–1832.
[71] Kaiyuan Zhang, Rong Chen, and Haibo Chen. 2015. NUMA-Aware Graph-Structured Analytics. *SIGPLAN Not.* 50, 8 (2015), 183–193.
[72] Yanfeng Zhang, Qixin Gao, Lixin Gao, and Cuirong Wang. 2014. Maiter: An Asynchronous Graph Processing Framework for Delta-Based Accumulative Iterative Computation. *TPDS* 25, 8 (2014), 2091–2100.
[73] Yunming Zhang, Mengjiao Yang, Riyadh Baghdadi, Shoaib Kamil, Julian Shun, and Saman Amarasinghe. 2018. Graphit: A high-performance graph DSL. *Proceedings of the ACM on Programming Languages* 2, OOPSLA (2018), 1–30.
[74] Kangfei Zhao and Jeffrey Xu Yu. 2017. All-in-one: graph processing in RDBMSs revisited. In *SIGMOD*. 1165–1180.
[75] Xiaowei Zhu, Wenguang Chen, Weimin Zheng, and Xiaosong Ma. 2016. Gemini: A computation-centric distributed graph processing system. In *USENIX OSDI*. 301–316.
[76] Xiaowei Zhu, Wentao Han, and Wenguang Chen. 2015. GridGraph: Large-Scale Graph Processing on a Single Machine Using 2-Level Hierarchical Partitioning. In *USENIX ATC*. 375–386.

A PROOF OF THEOREM 1

DSP. We study the decision problem of the scheduling problem, denoted by DSP and stated as follows:

- *Input*: Subgraphs $F_0, F_1, \ldots, F_{n-1}$, the cost function $C_{\mathcal{A}}$ (Equation 3), an m-core machine whose memory capacity is η and disk read bandwidth is γ, and a deadline B.
- *Question*: Does there exist a valid schedule $\mathcal{S}$ whose makespan is bounded by B, *i.e.,* $\max_{i\in[0,n)}\{t_i + C_{\mathcal{A}}(F_i, p_i)\} \le B$?

Proof of NP-completeness. We verify the upper bound of DSP by developing an NP algorithm as follows. The algorithm for DSP works as follows: (1) guess a schedule $\mathcal{S} = (\bar{p}, \bar{t})$; and (2) check whether the makespan $\max_{i\in[0,n)}\{t_i+C_{\mathcal{A}}(F_i, p_i)\} \le B$; if so, return `true`. The algorithm is clearly in NP since verification in step (2) can be done in polynomial time (PTIME); so is DSP.

We verify the lower bound of DSP by reduction from PARTITION problem, which is known to be NP-complete (cf. [28]). PARTITION is to decide, given a finite set A of positive integers, whether there exists a subset $A' \subseteq A$, such that A' and its complement $\bar{A}' = A \setminus A'$ have an equal sum, *i.e.,* $\sum_{i\in A'} a_i = \sum_{j\in\bar{A}'} b_j$.

Given a set of n positive integers $A = \{a_0, a_1, \ldots, a_{n-1}\}$, we construct a schedule $\mathcal{S}$ for a set of subgraphs $F_0, F_1, \ldots, F_{n-1}$, a positive integer m, two positive numbers η and γ, a deadline B, and a cost function $C_{\mathcal{A}}$ to ensure the following property: A can be partitioned into A' and $\bar{A}'$ of equal sum if and only if $\max_{i\in[0,n)}\{t_i + C_{\mathcal{A}}(F_i, p_i)\} \le B$. Without loss of generality, we assume $A' = \{a_0, a_1, \ldots, a_{k-1}\}$ and $\bar{A}' = \{a_k, a_{k+1}, \ldots, a_{n-1}\}$.

The construction details are:

(1) The cost function $C_{\mathcal{A}}$ is defined such that for all $i \in [0, n)$, $C_{\mathcal{A}}(F_i, 1) = C_{\mathcal{A}}(F_i, 2) = a_i$. More specifically, (a) $h^{\text{seq}}_{\mathcal{A}}(\bar{x}_i(v)) = 0.25$ and $h^{\text{para}}_{\mathcal{A}}(\bar{x}_i(v)) = 0.25$ are constants for any vertex v. (b) Fragment F_i is constructed as a collection of a_i connected vertex pairs. That is, F_i has a_i pairs of vertices. For an undirected graph, there exists an edge between each pair of vertices; for a direct graph, each vertex in the pair has an outgoing edge to the other. As a result, the average degree d_i of F_i is 1. One can easily verify from Equation 3 that $C_{\mathcal{A}}(F_i, 1) = C_{\mathcal{A}}(F_i, 2) = a_i$ for all $i \in [0, n)$.

(2) $m = 2$ and $\eta = \max_{|K|=\min\{4,n\}} \sum_{K\subseteq[0,n)} s(F_i)$. Intuitively, the machine has two cores (*e.g.,* Core 0 and Core 1), and four largest fragments can fit into the memory at the same time. We also set $\gamma = \infty$, *i.e.,* loading time for a fragment is negligible.

(3) Schedule $\mathcal{S}$ assigns $p_i = 1$ for all $i \in [0, n)$. It sets the start time $t_0 = t_k = 0$, and $t_i = t_{i-1} + a_{i-1}$ for all $0 < i < k$ and $k < i < n$. In other words, fragments are partitioned into two groups $G_0 = \{F_0, F_1, \ldots F_{k-1}\}$ and $G_1 = \{F_k, F_{k+1}, \ldots F_{n-1}\}$. Each fragment in G_α is executed one after another on Core α, for $\alpha \in \{0, 1\}$.

(4) $B = \frac{1}{2}\sum_{a\in A} a$. Note that we assume *w.l.o.g.* that B is a positive integer and thus $\sum_{a\in A} a = 2B$.

We next verify the correctness of our reduction.

($\Rightarrow$) Suppose that A can be partitioned into A' and $\bar{A}'$ of equal sum. We have that $\sum_{a\in A'} a = \sum_{a\in\bar{A}'} a = B$. As a result, the makespan of schedule $\mathcal{S}$ is

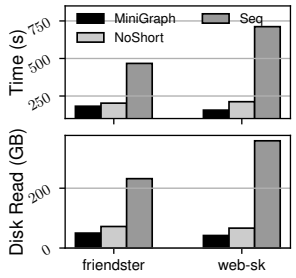

Figure 8: PR: 50% memory budget.

Metric	SSSP		WCC		PR	
	MiniGraph	GridGraph	MiniGraph	GridGraph	MiniGraph	GridGraph
# Supersteps	**18**	68	**16**	199	20	20
Disk Read (GB)	**2007**	3471.4	**1843.2**	4275.9	**1105.92**	2048
Shortcut I/O (GB)	184.4	N/A	655.36	N/A	245.8	N/A
Average CPU Utilization	**18%**	3.1%	**19.8%**	4.1%	**55.3%**	10.1%
I/O-Compute Correlation	**-0.048**	-0.222	**0.021**	-0.093	-0.047	**0.029**
Cache Hit Rate	**53.27%**	50.13%	**55.38%**	53.66%	**69.37%**	63.28%

Table 5: Runtime statistics for SSSP, WCC and PR over `clueWeb`.

$$\begin{aligned}\max_{i\in[0,n)}\{t_i + C_{\mathcal{A}}(F_i, p_i)\} &= \max\{t_{k-1} + a_{k-1}, t_{n-1} + a_{n-1}\}\\ &= \max\{\Sigma_{i=0}^{k-1} a_i, \Sigma_{j=k}^{n-1} a_j\}\\ &= \max\{B, B\} = B.\end{aligned}$$

($\Leftarrow$) Suppose that the makespan of schedule $\mathcal{S}$ can meet deadline B, *i.e.,* $\max_{i\in[0,n)}\{t_i + C_{\mathcal{A}}(F_i, p_i)\} \le B$. We have $\max\{\Sigma_{i=0}^{k-1} a_i, \Sigma_{j=k}^{n-1} a_j\} \le B$. As a result,

$$\Sigma_{i=0}^{k-1} a_i \le B, \tag{5}$$

$$\Sigma_{j=k}^{n-1} a_j \le B. \tag{6}$$

Here we construct $A' = \{a_0, a_1, \ldots, a_{k-1}\}$ and its complement $\bar{A}' = \{a_k, a_{k+1}, \ldots, a_{n-1}\}$. From Equation 5 and Equation 6, we have $\Sigma_{a\in A'} a \le B$ and $\Sigma_{b\in\bar{A}'} b \le B$, respectively. Provided that B is defined such that $\sum_{a\in A} a = 2B$, we have $\Sigma_{a\in A'} a = \Sigma_{b\in\bar{A}'} b = B$. In other words, A' and its complement $\bar{A}'$ have an equal sum B.

B ADDITIONAL EXPERIMENTAL RESULTS

Below we report additional experimental results.

B.1 Out-of-Core Efficiency

This section shows some additional results for PR.

PageRank. Figure 8 shows the performance of MiniGraph and its variants for PR, on `friendster` and `web-sk`. We find the following.

(1) Compared to $\text{MiniGraph}_{\text{NoShort}}$, on average MiniGraph is 11.2% and 35.9% faster over the two graphs, respectively. Moreover, shortcuts are much more effective on `web-sk` than on `friendster`. The reasons include the following: (a) `web-sk` has more connected components. Its largest connected component has 70.85% vertices, and 13.63% vertices are dangling nodes that are not connected to any other vertex. Under PR, some parts of the graph may already converge while other parts still require iterative computations. This improves the opportunity for shortcut (A) (Section 6). (b) On the contrary, `friendster` has a single large connected component only.

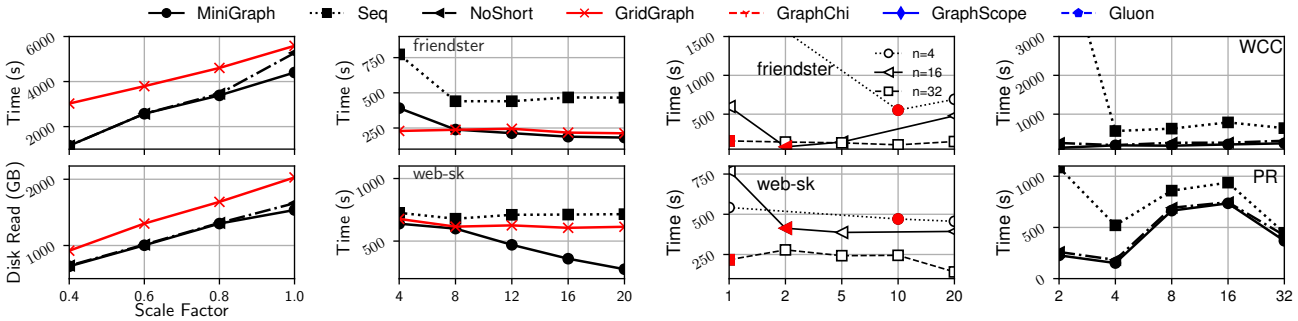

(a) Varying $|G|$: PR. (b) Varying m: WCC. (c) Varying p_i: PR. (d) Varying n: `friendster`.

Figure 9: Scalability of MiniGraph.

As a result, PR actively updates the ranking cores of *all* vertices in *every* superstep, which effectively invalidates both Shortcuts (A) and (C). Out of the three shortcuts listed in Section 6, Shortcut (B) is the only one that can be actively exploited.

(2) MiniGraph is significantly faster than $\text{MiniGraph}_{\text{Seq}}$. It is 156.6% and 455.9% faster over `friendster` and `web-sk`, respectively. This is because of the VC nature of PR. It programs independent and massively parallelizable operations on individual vertices and edges; therefore, it would under-utilize the multi-core parallelism if intra-subgraph parallelism cannot be exploited on a single machine.

Performance over `clueWeb`. Table 5 shows runtime statistics for some applications over `clueWeb`. The raw graph is 137GB large; it way exceeds the physical memory capacity (47% of `clueWeb`) of our workstation testbed. That said, we no longer use `cgroups` to enforce a "software" memory budget in this experiment.

As shown in Table 4, MiniGraph is on average 4.59×, 4.25× and 2.1× faster than GridGraph for SSSP, WCC and PR, respectively. Table 5 further reports the number of supersteps, the volume of disk read traffic, I/O reduction from shortcuts, the average CPU utilization, the correlation coefficient r between real-time I/O and CPU usage, and the CPU cache hit rate.

The results are consistent with applications over `web-sk`, another Web graph evaluated in Section 7. On average, (1) for SSSP, and WCC, MiniGraph reduces the BSP supersteps by 73.5%, and 91.9%, respectively. (2) Compared to GridGraph, MiniGraph induces 42.2%, 56.89%, and 46% less disk read traffic, in which shortcut optimizations contribute 5.3%, 15.3%, and 12% for SSSP, WCC, and PR, respectively. (3) Compared to GridGraph, MiniGraph improves CPU utilization by 14.9%–45.2%.

B.2 Scalability

Under 50% memory budget, we present additional experimental results on the scalability of MiniGraph.

Varying $|G|$ for PageRank. As shown in Figure 9a when varying the scaling factor δ from 0.4 to 1.0 and G is `clueWeb`, (1) MiniGraph scales well with $|G|$. It takes 1.7× longer, while it is 1.8× for GridGraph. (2) MiniGraph also scales better than its variants. $\text{MiniGraph}_{\text{NoShort}}$ increases 4.6× when δ varies from 0.4 to 1.0. These further verify the effectiveness of our optimization strategies. (3) When $|G|$ grows 2.5×, MiniGraph induces only 2.2× I/O traffic, a large part due to the shortcut optimizations.

Varying m for WCC. Varying the number m of cores from 4 to 20, we ran WCC over `friendster` and `web-sk`. As shown in Figure 9b, (1) MiniGraph scales sub-linearly with m on both graphs. When varying m from 4 to 20, its performance improves 2.1× and 2.3× over `friendster` and `web-sk`, respectively. (2) It scales better than GridGraph, which does not improve much (up to +2.1% over `friendster` and +29.7% over `web-sk`) when m varies from 4 to 20. This is because GridGraph is always I/O-bound, which echoes with our findings in Figure 6b. (3) It also scales better than $\text{MiniGraph}_{\text{Seq}}$, whose performance barely improves when $m \leq 8$ due to the lack of intra-subgraph parallelism. This further justifies the need for a hybrid parallel model that supports both GC and VC.

Varying p_i for PageRank. Besides testing the impact of varying p_i for WCC (see Figure 6g), Figure 9c reports its impact on PR over both `friendster` and `web-sk`. For each graph partitioning, we mark its tentative allocation $\hat{p}_i$ (Section 5) with colored points. The results show that for PR, our simple heuristic algorithm for deciding $\hat{p}_i$ again selects a near-optimal value for p_i. It further verifies that MiniGraph strikes a balance between the two levels of parallelism and improves the overall multi-core parallelism.

Varying n over `friendster`. In addition to experiments with different partitioning of `web-sk` (see Figure 6h), we also tested the impact of n over `friendster`. Varying the number n of partitions from 2 to 64, Figure 9d shows the performance of WCC and PR.

(1) For VC-based PR, its optimal n is also 4 (consistent with results over `web-sk`). It suggests that regardless of the graph distribution, VC algorithms with massively parallelizable operations always prefer exploiting intra-subgraph parallelism to inter-subgraph parallelism in MiniGraph. This is reasonable: a higher inter-subgraph parallelism often leads to a more fragmented graph, which generates more message updates across supersteps, inducing more undesirable computational overheads for message aggregation.

(2) For GC-based WCC, the optimal n is 4. This shows a pattern similar to the one over `web-sk`. It verifies the complexity of deciding an optimal n, which we leave as future work.